

12

Resonant Cavities and Waveguides

This chapter initiates our study of resonant accelerators. The category includes rf (radio-frequency) linear accelerators, cyclotrons, microtrons, and synchrotrons. Resonant accelerators have the following features in common:

1. Applied electric fields are harmonic. The continuous wave (CW) approximation is valid; a frequency-domain analysis is the most convenient to use. In some accelerators, the frequency of the accelerating field changes over the acceleration cycle; these changes are always slow compared to the oscillation period.
2. The longitudinal motion of accelerated particles is closely coupled to accelerating field variations.
3. The frequency of electromagnetic oscillations is often in the microwave regime. This implies that the wavelength of field variations is comparable to the scale length of accelerator structures. The full set of the Maxwell equations must be used.

Microwave theory relevant to accelerators is reviewed in this chapter. Chapter 13 describes the coupling of longitudinal particle dynamics to electromagnetic waves and introduces the concept of phase stability. The theoretical tools of this chapter and Chapter 13 will facilitate the study of specific resonant accelerators in Chapters 14 and 15.

As an introduction to frequency-domain analysis, Section 12.1 reviews complex exponential representation of harmonic functions. The concept of complex impedance for the analysis of passive element circuits is emphasized. Section 12.2 concentrates on a lumped element model for

Resonant Cavities and Waveguides

the fundamental mode of a resonant cavity. The Maxwell equations are solved directly in Section 12.3 to determine the characteristics of electromagnetic oscillations in resonant cavities. Attention is centered on the TM_{010} mode because it is the most useful mode for particle acceleration. Physical properties of resonators are discussed in Section 12.4. Subjects include the Q value of a cavity and effects of competing modes. Methods of extracting energy from and coupling energy to resonant cavities are discussed in Section 12.5.

Section 12.6 develops the frequency-domain analysis of transmission lines. There are three reasons to extend the analysis of transmission lines. First, an understanding of transmission lines helps to illuminate properties of resonant cavities and waveguides. Second, transmission lines are often used to transmit power to accelerator cavities. Finally, the transmission line equations illustrate methods to match power sources to loads with reactive components, such as resonant cavities. In this application, a transmission line acts to transform the impedance of a single-frequency input. Section 12.7 treats the cylindrical resonant cavity as a radial transmission line with an open-circuit termination at the inner radius and a short-circuit termination at the outer radius.

Section 12.8 reviews the theory of the cylindrical waveguide. Waveguides are extended hollow metal structures of uniform cross section. Traveling waves are contained and transported in a waveguide; the frequency and field distribution is determined by the shape and dimensions of the guide. A lumped circuit element model is used to demonstrate approximate characteristics of guided wave propagation, such as dispersion and cutoff. The waveguide equations are then solved exactly.

The final two sections treat the topic of slow-wave structures, waveguides with boundaries that vary periodically in the longitudinal direction. They transport waves with phase velocity equal to or less than the speed of light. The waves are therefore useful for continuous acceleration of synchronized charged particles. A variety of models are used to illustrate the physics of the iris-loaded waveguide, a structure incorporated in many traveling wave accelerators. The interpretation of dispersion relationships is discussed in Section 12.10. Plots of frequency versus wavenumber yield the phase velocity and group velocity of traveling waves. It is essential to determine these quantities in order to design high-energy resonant accelerators. As an example, the dispersion relationship of the iris-loaded waveguide is derived.

12.1 COMPLEX EXPONENTIAL NOTATION AND IMPEDANCE

Circuits consisting of a harmonic voltage source driving resistors, capacitors, and inductors, are described by an equation of the form

$$\alpha (di/dt) + \beta i + \gamma \int i dt = V_0 \cos \omega t. \quad (12.1)$$

The solution of Eq. (12.1) has homogeneous and particular parts. Transitory behavior must

Resonant Cavities and Waveguides

include the homogenous part. Only the particular part need be included if we restrict our attention to CW (continuous wave) excitation. The particular solution has the form

$$i(t) = I_0 \cos(\omega t + \phi). \quad (12.2)$$

I_0 and ϕ depend on the magnitude of the driving voltage, the elements of the circuit, and ω . Because Eq. (12.1) describes a physical system, the solution must reflect a physical answer. Therefore, I_0 and ϕ are real numbers. They can be determined by direct substitution of Eq. (12.2) into Eq. (12.1). In most cases, this procedure entails considerable manipulation of trigonometric identities.

The mathematics to determine the particular solution of Eq. (12.1) and other circuit equations with a single driving frequency can be simplified considerably through the use of the complex exponential notation for trigonometric functions. In using complex exponential notation, we must remember the following facts:

1. All physical problems must have an answer that is a real number. Complex numbers have no physical meaning.
2. Complex numbers are a convenient mathematical method for handling trigonometric functions. In the solution of a physical problem, complex numbers can always be grouped to form real numbers.
3. The answers to physical problems are often written in terms of complex numbers. This convention is used because the results can be written more compactly and because there are well-defined rules for extracting the real-number solution.

The following equations relate complex exponential functions to trigonometric functions:

$$\cos \omega t = [\exp(j\omega t) + \exp(-j\omega t)]/2, \quad (12.3)$$

$$\sin \omega t = [\exp(j\omega t) - \exp(-j\omega t)]/2j. \quad (12.4)$$

where $j = \sqrt{-1}$. The symbol j is used to avoid confusion with the current, i . The inverse relationship is

$$\exp(j\omega t) = \cos \omega t + j \sin \omega t. \quad (12.4)$$

In Eq. (12.1), the expression $V_0[\exp(j\omega t) + \exp(-j\omega t)]/2$ is substituted for the voltage, and the current is assumed to have the form

$$i(t) = A \exp(j\omega t) + B \exp(-j\omega t). \quad (12.5)$$

Resonant Cavities and Waveguides

The coefficients A and B may be complex numbers if there is a phase difference between the voltage and the current. They are determined by substituting Eq. (12.6) into Eq. (12.1) and recognizing that the terms involving $\exp(j\omega t)$ and $\exp(-j\omega t)$ must be separately equal if the solution is to hold at all times. This procedure yields

$$A = (j\omega V_0/2) / (-\alpha\omega^2 + j\omega\beta + \gamma), \quad (12.7)$$

$$B = (-j\omega V_0/2) / (-\alpha\omega^2 - j\omega\beta + \gamma). \quad (12.8)$$

The complex conjugate of a complex number is the number with $-j$ substituted for j . Note that B is the complex conjugate of A . The relationship is denoted $B = A^*$.

Equations (12.7) and (12.8) represent a formal mathematical solution of the problem; we must rewrite the solution in terms of real numbers to understand the physical behavior of the system described by Eq. (12.1). Expressing Eq. (12.2) in complex notation and setting the result equal to Eq. (12.6), we find that

$$A\exp(j\omega t) + A^*\exp(-j\omega t) = I_0 [\exp(j\omega t)\exp(\varphi) + \exp(-j\omega t)\exp(-\varphi)]/2. \quad (12.9)$$

Terms involving $\exp(j\omega t)$ and $\exp(-j\omega t)$ must be separately equal. This implies that

$$A = I_0 \exp(j\varphi)/2 = I_0 (\cos\varphi + j\sin\varphi)/2 \quad (12.10)$$

by Eq. (12.5). The magnitude of the real solution is determined by multiplying Eq. (12.10) by its complex conjugate:

$$A \cdot A^* = I_0^2 (\cos\varphi + j\sin\varphi)/2,$$

or

$$I_0 = 2 \sqrt{A \cdot A^*}. \quad (12.11)$$

Inspection of Eq. (12.10) shows that the phase shift is given by

$$\varphi = \tan^{-1}[Im(A)/Re(A)]. \quad (12.12)$$

Returning to Eq. (12.1), the solution is

Resonant Cavities and Waveguides

$$I_0 = V_0 \omega / \sqrt{(\gamma - \alpha \omega^2)^2 + \omega^2 \beta^2},$$

$$\phi = \tan^{-1}(\gamma - \alpha \omega^2) / \omega \beta.$$

This is the familiar resonance solution for a driven, damped harmonic oscillator.

Part of the effort in solving the above problem was redundant. Because the coefficient of the second part of the solution must equal the complex conjugate of the first, we could have used a trial solution of the form

$$i(t) = A \exp(j\omega t). \quad (12.13)$$

We arrive at the correct answer if we remember that Eq. (12.13) represents only half of a valid solution. Once A is determined, the real solution can be extracted by applying the rules of Eq. (12.11) and (12.12). Similarly, in describing an electromagnetic wave traveling in the $+z$ direction, we will use the form $E \sim E_0 \exp[j(\omega t - kz)]$. The form is a shortened notation for the function $E \sim E_0 \exp[j(\omega t - kz)] + E_0^* \exp[-j(\omega t - kz)] \sim E_0 \cos(\omega t - kz + \phi)$ where E_0 is a real number. The function for a wave traveling in the negative z direction is abbreviated $E \sim E_0 \exp[j(\omega t + kz)]$. Complex exponential notation is useful for solving lumped element circuits with CW excitation. In this circumstance, voltages and currents in the circuit vary harmonically at the driving frequency and differ only in amplitude and phase. In complex exponential notation, the voltage and current in a section of a circuit are related by

$$V/I = Z. \quad (12.14)$$

The quantity Z , the impedance, is a complex number that contains information on amplitude and phase. Impedance is a function of frequency.

The impedance of a resistor R is simply

$$Z_R = R. \quad (12.15)$$

A real impedance implies that the voltage and current are in phase as shown in Figure 12.1a. The time-averaged value of VI through a resistor is nonzero; a resistor absorbs energy.

The impedance of a capacitor can be calculated from Eq. (9.5). If the voltage across the capacitor is

$$V(t) = V_0 \cos \omega t, \quad (12.16)$$

then the current is

Resonant Cavities and Waveguides

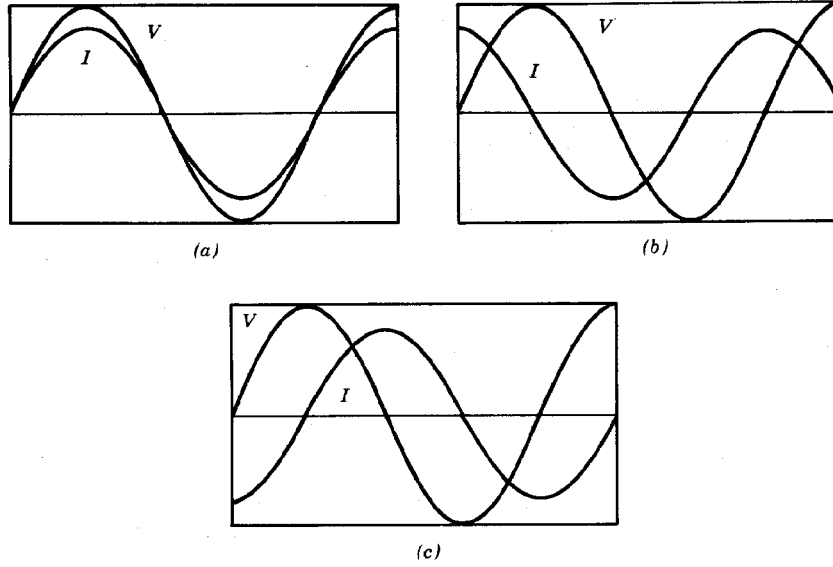


Figure 12.1 Variations of voltage and current in simple circuit elements driven at single frequency. (a) Resistor. (b) Capacitor. (c) Inductor.

$$i(t) = C \, dV/dt = -\omega C V_0 \sin \omega t = \omega C V_0 \cos(\omega t + \pi/2). \quad (12.17)$$

Equation (12.17) specifies the magnitude and amplitude of voltage across versus current through a capacitor. There is a 90° phase shift between the voltage and current; the current leads the voltage, as shown in Figure 12.1b. The capacitor is a reactive element; the time average of $V(t)i(t)$ is zero. In complex exponential notation, the impedance can be expressed as a single complex number

$$Z_C = (1/\omega C) \exp(j\pi/2) = -j/\omega C \quad (12.18)$$

if the convention of Eq. (12.13) is adopted. The impedance of a capacitor has negative imaginary part. This implies that the current leads the voltage. The impedance is inversely proportional to frequency; a capacitor acts like a short circuit at high frequency.

The impedance of an inductor can be extracted from the equation $V(t) = L \, di(t)/dt$. Again, taking voltage in the form of Eq. (12.16), the current is

$$i(t) = \frac{V_0 \sin \omega t}{\omega L} = \frac{V_0 \cos(\omega t - \pi/2)}{\omega L}.$$

The current lags the voltage, as shown in Figure 12.1c. The complex impedance of an inductor is

$$Z_l = j\omega L. \quad (12.19)$$

The impedance of an inductor is proportional to frequency; inductors act like open circuits at high frequency.

12.2 LUMPED CIRCUIT ELEMENT ANALOGY FOR A RESONANT CAVITY

A resonant cavity is a volume enclosed by metal walls that supports an electromagnetic oscillation. In accelerator applications, the oscillating electric fields accelerate charged particles while the oscillating magnetic fields provide inductive isolation. To initiate the study of electromagnetic oscillations, we shall use the concepts developed in the previous section to solve a number of lumped element circuits. The first, shown in Figure 12.2, illustrates the process of inductive isolation in a resonant circuit. A harmonic voltage generator with output $V(t) = V_0 \exp(j\omega t)$ drives a parallel combination of a resistor, capacitor, and inductor. Combinations of impedances are governed by the same rules that apply to parallel and series combinations of resistors. The total circuit impedance at the voltage generator is

$$Z(\omega) = V_0 \exp(j\omega t) / I_0 \exp(j\omega t) = (1/Z_r + 1/Z_C + 1/Z_L)^{-1}. \quad (12.20)$$

The quantity I_0 is generally a complex number.

Consider the part of the circuit of Figure 12.2 enclosed in dashed lines: a capacitor in parallel with an inductor. The impedance is

$$Z(\omega) = (j\omega C + 1/j\omega L)^{-1} = j\omega L / (1 - \omega^2 LC). \quad (12.21)$$

The impedance is purely imaginary; therefore, the load is reactive. At low frequency ($\omega < 1/\sqrt{LC}$) the impedance is positive, implying that the circuit is inductive. In other words, current flow through the inductor dominates the behavior of the circuit. At high frequency, the

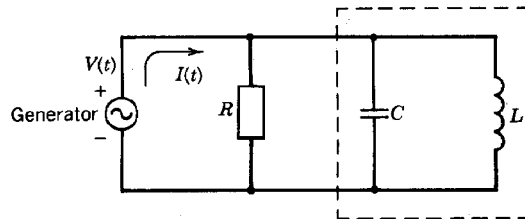


Figure 12.2 Driven RLC circuit with shunt resistance. Reactive section of circuit indicated by dashed line.

Resonant Cavities and Waveguides

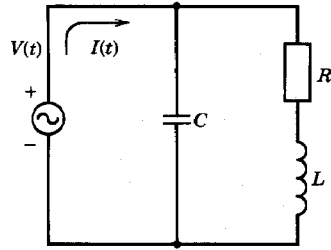


Figure 12.3 Driven RLC circuit; inductor with series resistance.

impedance is negative and the circuit acts as a capacitive load. When $\omega = \omega_0 = 1/\sqrt{LC}$, the impedance of the combined capacitor and inductor becomes infinite. This condition is called *resonance*; the quantity ω_0 is the resonant frequency. In this circumstance, the reactive part of the total circuit of Figure 12.2 draws no current when a voltage is applied across the resistor. All current from the generator flows into the resistive load. The reactive part of the circuit draws no current at $\omega = \omega_0$ because current through the inductor is supplied completely by displacement current through the capacitor. At resonance, the net current from the generator is minimized for a given voltage. This is the optimum condition for energy transfer if the generator has nonzero output impedance.

The circuit of Figure 12.3 illustrates power losses in resonant circuits. Again, an inductor and capacitor are combined in parallel. The difference is that the inductor is imperfect. There are resistive losses associated with current flow. The losses are represented by a series resistor. The impedance of the circuit is

$$Z(\omega) = [j\omega C + 1/(j\omega L + R)]^{-1} = [j\omega L + R] / [(1 - \omega^2 LC) + j\omega RC].$$

Converting the denominator in the above equation to a real number, we find that the magnitude of the impedance is proportional to

$$Z(\omega) \sim 1/[(1 - \omega^2/\omega_0^2)^2 + (\omega RC)^2]. \quad (12.22)$$

Figure 12.4 shows a plot of total current flowing in the reactive part of the circuit versus current input from the generator. Two cases are plotted: resonant circuits with low damping and high damping. Note that the impedance is no longer infinite at $\omega = 1/\sqrt{LC}$. For a cavity with resistive losses, power must be supplied continuously to support oscillations. A circuit is in resonance when large reactive currents flow in response to input from a harmonic power generator. In other words, the amplitude of electromagnetic oscillations is high. Inspection of Figure 12.4 and Eq. (12.22) shows that there is a finite response width for a driven damped resonant circuit. The frequency width, $\Delta\omega = \omega - \omega_0$, to reduce the peak impedance by a factor of 5 is

Resonant Cavities and Waveguides

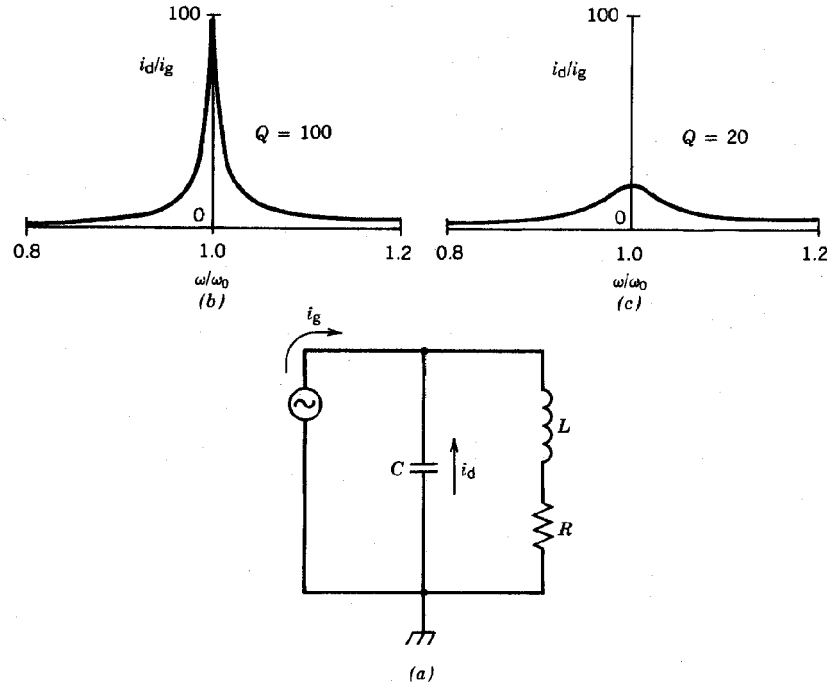


Figure 12.4 Resonant drive of RLC circuit. (a) Circuit diagram; circle represents ac generator. (b) Ratio of reactive current to current input from generator (i_d/i_g); $Q = 100$. (c) i_d/i_g ; $Q = 20$.

$$\frac{\Delta\omega}{\omega_0} \approx \frac{R}{\sqrt{LC}}. \quad (12.23)$$

Resonant circuits are highly underdamped; therefore, $\Delta\omega/\omega \ll 1$.

Resonant circuit damping is parametrized by the quantity Q . The circuit Q is defined as

$$\begin{aligned} Q &= \frac{\omega_0 \text{ (energy stored in the resonant circuit)}}{\text{(time-averaged power loss)}} \\ &= \frac{\pi \text{ (energy stored in the resonant circuit)}}{\text{(energy lost per half cycle)}} \end{aligned} \quad (12.24)$$

In the limit of low damping near resonance, the reactive current exchanged between the inductor and capacitor of the circuit of Figure 12.3 is much larger than the current input from the generator. The reactive current is $i(t) = I_0 \exp(j\omega t)$, where I_0 is a slowly decreasing function of time. The circuit energy, U , is equal to the energy stored in the inductor at peak current:

Resonant Cavities and Waveguides

$$U = LI_0 I_0^* / 2 \quad (12.25)$$

Energy is lost to the resistor. The power lost to the resistor (averaged over a cycle) is

$$\overline{P} = \overline{i(t)^2} R = \frac{1}{2} I_0 I_0^* R. \quad (12.26)$$

Substituting Eqs. (12.25) and (12.26) into Eq. (12.24), the Q value for the LRC circuit of Figure 12.3 is

$$Q \cong \omega_0 L / R = \sqrt{L/C} / R. \quad (12.27)$$

In an underdamped circuit, the characteristic impedance of the LC circuit is large compared to the resistance, so that $Q \gg 1$.

Energy balance can be used to determine the impedance that the circuit of Figure 12.3 presents to the generator at resonance. The input voltage V_0 is equal to the voltage across the capacitor. The input voltage is related to the stored energy in the circuit by

$$U = CV_0^2 / 2 = V_0^2 / 2\omega_0 \sqrt{L/C}. \quad (12.28)$$

By the definition of Q , the input voltage is related to the average power loss by

$$\overline{P} = V_0^2 / 2Q\sqrt{L/C}. \quad (12.29)$$

Defining the resistive input impedance so that

$$\overline{P} = \overline{V^2(t)} / R_{in} = V_0^2 / 2R_{in}, \quad (12.30)$$

we find at resonance ($\omega \cong \omega_0$) that

$$R_{in} \cong Q \sqrt{L/C} = (\sqrt{L/C})^2 / R. \quad (12.31)$$

The same result can be obtained directly from the general impedance expression in the limit $\sqrt{L/C} \gg R$. The impedance is much larger than R . This reflects the fact that the reactive current is much larger than the current from the generator. In terms of Q , the resonance width of an

Resonant Cavities and Waveguides

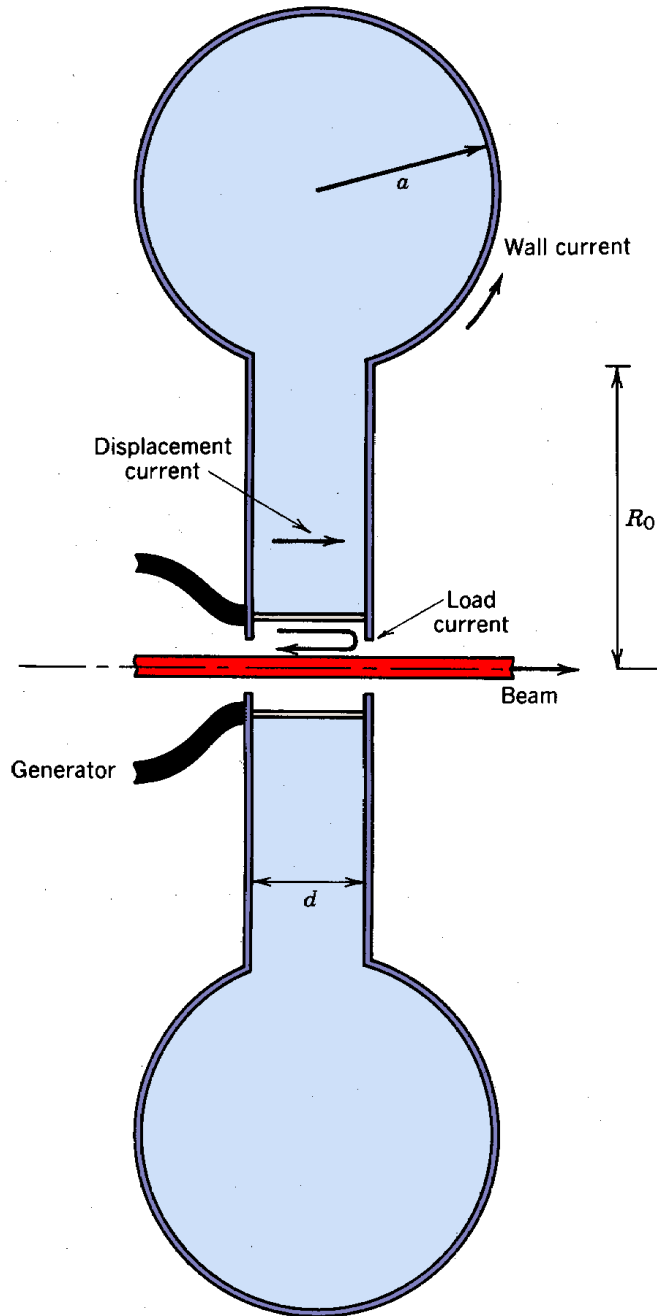


Figure 12.5 Reentrant cavity with on-axis power input.

imperfect oscillating circuit [Eq. (12.23)] can be written

$$\Delta\omega/\omega_0 \cong 1/Q. \quad (12.32)$$

Resonant Cavities and Waveguides

Resonant cavities used for particle acceleration have many features in common with the circuits we have studied in this section. Figure 12.5 illustrates a particularly easy case to analyze, the reentrant cavity. This cavity is used in systems with space constraints, such as klystrons. It oscillates at relatively low frequency for its size. The reentrant cavity can be divided into predominantly capacitive and predominantly inductive regions. In the central region, there is a narrow gap. The capacitance is large and the inductance is small. A harmonic voltage generator connected at the center of the cavity induces displacement current. The enlarged outer region acts as a single-turn inductor. Real current flows around the wall to complete the circuit. If the walls are not superconducting, the inductor has a series resistance.

Assume that there is a load, such as a beam, on the axis of the cavity. Neglecting cavity resistance, the circuit is the same as that of Figure 12.2. If the generator frequency is low, most of the input current flows around the metal wall (leakage current). The cavity is almost a short circuit. At high frequency, most of the current flows across the capacitor as displacement current. At the resonance frequency of the cavity, the cavity impedance is infinite and all the generator energy is directed into the load. In this case, the cavity can be useful for particle acceleration. When the cavity walls have resistivity, the cavity acts as a high impedance in parallel to the beam load. The generator must supply energy for cavity losses as well as energy to accelerate the beam.

The resonant cavity accelerator has much in common with the cavity of an induction linear accelerator. The goal is to accelerate particles to high energy without generating large electrostatic voltages. The outside of the accelerator is a conductor; voltage appears only on the beamline. Electrostatic voltage is canceled on the outside of the accelerator by inductively generated fields. The major difference is that leakage current is inhibited in the induction linear accelerator by ferromagnetic inductors. In the resonant accelerator, a large leakage current is maintained by reactive elements. The linear induction accelerator has effective inductive isolation over a wide frequency range; the resonant accelerator operates at a single frequency. The voltage on the axis of a resonant cavity is bipolar. Therefore, particles are accelerated only during the proper half-cycle. If an accelerator is constructed by stacking a series of resonant cavities, the crossing times for particles must be synchronized to the cavity oscillations.

The resonant frequency of the reentrant cavity can be estimated easily. Dimensions are illustrated in Figure 12.5. The capacitance of the central region is $C \cong \epsilon_o \pi R_0^2/d$, and the inductance is $L \cong \mu_o \pi a^2/2\pi(R_0+a)$. The resonant angular frequency is

$$\omega_0 = 1/\sqrt{LC} \cong \sqrt{2\pi(R_0+a)d/\epsilon_o \mu_o R_0^2 a^2 \pi^2} = c \sqrt{2(R_0+a)d/R_0^2 a^2 \pi}. \quad (12.33)$$

12.3 RESONANT MODES OF A CYLINDRICAL CAVITY

The resonant modes of a cavity are the natural modes for electromagnetic oscillations. Once excited, a resonant mode will continue indefinitely in the absence of resistivity with no further input of energy. In this section, we shall calculate modes of the most common resonant structure

Resonant Cavities and Waveguides

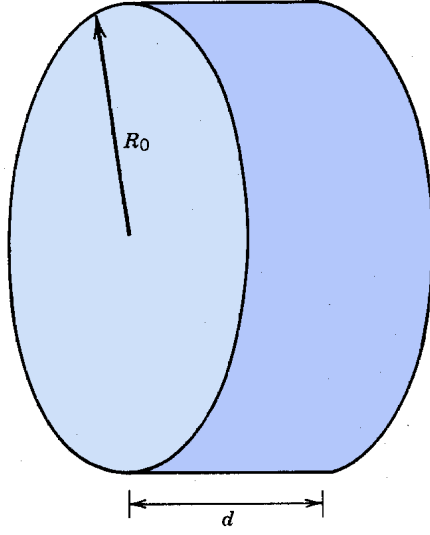


Figure 12.6 Geometry of cylindrical resonant cavity.

encountered in particle accelerator applications, the cylindrical cavity (Fig. 12.6). The cavity length is denoted d and radius R_0 . In the initial treatment of resonant modes, we shall neglect the perturbing effects of power feeds, holes for beam transport, and wall resistivity. The cylindrical cavity has some features in common with the reentrant cavity of Section 2.2. A capacitance between the upstream and downstream walls carries displacement current. The circuit is completed by return current along the walls. Inductance is associated with the flow of current. The main difference from the reentrant cavity is that regions of electric field and magnetic field are intermixed. In this case, a direct solution of the Maxwell equations is more effective than an extension of the lumped element analogy. This approach demonstrates that resonant cavities can support a variety of oscillation modes besides the low-frequency mode that we identified for the reentrant cavity.

We seek solutions for electric and magnetic fields that vary in time according to $\exp(j\omega t)$. We must use the full set of coupled Maxwell equations [Eqs. (3.11)-(3.14)]. We allow the possibility of a uniform fill of dielectric or ferromagnetic material; these materials are assumed to be linear, characterized by parameters ϵ and μ . The field equations are

$$\nabla \times \mathbf{E} + \partial \mathbf{B} / \partial t = 0, \quad (12.34)$$

$$\nabla \cdot \mathbf{E} = 0, \quad (12.35)$$

$$\nabla \times \mathbf{B} - \epsilon \mu \partial \mathbf{E} / \partial t = 0, \quad (12.36)$$

$$\nabla \cdot \mathbf{B} = 0. \quad (12.37)$$

Applying the vector identity $\nabla \times (\nabla \times \mathbf{V}) = \nabla(\nabla \cdot \mathbf{V}) - \nabla^2 \mathbf{V}$, Eqs. (12.34)-(12.37) can be rewritten as

Resonant Cavities and Waveguides

$$\nabla^2 \mathbf{E} - (1/v^2) \partial^2 \mathbf{E} / \partial t^2 = 0, \quad (12.38)$$

$$\nabla^2 \mathbf{B} - (1/v^2) \partial^2 \mathbf{B} / \partial t^2 = 0. \quad (12.39)$$

where v is the velocity of light in the cavity medium,

$$v = c / \sqrt{\epsilon \mu / \epsilon_0 \mu_0}. \quad (12.40)$$

The features of electromagnetic oscillations can be found by solving either Eq. (12.38) or (12.39) for \mathbf{E} or \mathbf{B} . The associated magnetic or electric fields can then be determined by substitution into Eq. (12.34) or (12.36). Metal boundaries constrain the spatial variations of fields. The wave equations have solutions only for certain discrete values of frequency. The values of resonant frequencies depend on how capacitance and inductance are partitioned in the mode.

The general solutions of Eqs. (12.38) and (12.39) in various cavity geometries are discussed in texts on electrodynamics. We shall concentrate only on resonant modes of a cylindrical cavity that are useful for particle acceleration. We shall solve Eq. (12.38) for the electric field since there are easily identified boundary conditions. The following assumptions are adopted:

1. Modes of interest have azimuthal symmetry ($\partial/\partial\theta = 0$).
2. The electric field has no longitudinal variation, or $\partial \mathbf{E} / \partial z = 0$.
3. The only component of electric field is longitudinal, E_z .
4. Fields vary in time as $\exp(j\omega t)$.

The last two assumptions imply that the electric field has the form

$$\mathbf{E} = E_z(r) \exp(j\omega t) \mathbf{u}_z. \quad (12.41)$$

Using the cylindrical coordinate form of the Laplacian operator, dropping terms involving azimuthal and longitudinal derivatives, and substituting Eq. (12.41), we find that the class of resonant modes under consideration satisfies the equation

$$\frac{d^2 E_z(r)}{dr^2} + \frac{1}{r} \frac{dE_z(r)}{dr} + \frac{\omega^2}{v^2} E_z(r) = 0. \quad (12.42)$$

Equation (12.42) is expressed in terms of total derivatives because there are only radial variations. Equation (12.42) is a special form of the Bessel equation. The solution can be expressed in terms

Resonant Cavities and Waveguides

TABLE 12.1 Parameters of TM_{0n0} Modes

Mode	k_n	ω_n
TM_{010}	$2.405/R_0$	$2.405/\sqrt{\epsilon\mu} R_0$
TM_{020}	$5.520/R_0$	$5.520/\sqrt{\epsilon\mu} R_0$
TM_{030}	$8.654/R_0$	$8.654/\sqrt{\epsilon\mu} R_0$
TM_{040}	$11.792/R_0$	$11.792/\sqrt{\epsilon\mu} R_0$

of the zero-order Bessel functions, $J_0(k_n r)$ and $Y_0(k_n r)$. The Y_0 function is eliminated by the requirement that E_z has a finite value on the axis. The solution is

$$E_{zn}(r, t) = E_{0n} J_0(k_n r) \exp(j\omega t), \quad (12.43)$$

where E_{0n} is the magnitude of the field on the axis.

The second boundary condition is that the electric field parallel to the metal wall at $r = R_0$ must be zero, or $E_z(R_0, t) = 0$. This implies that only certain values of k_n give valid solutions. Allowed values of k_n are determined by the zeros of J_0 (Table 12.1). A plot of $E_z(r)$ for $n = 1$ is given in Figure 12.7. Substituting Eq. (12.43) into Eq. (12.42), the angular frequency is related to the

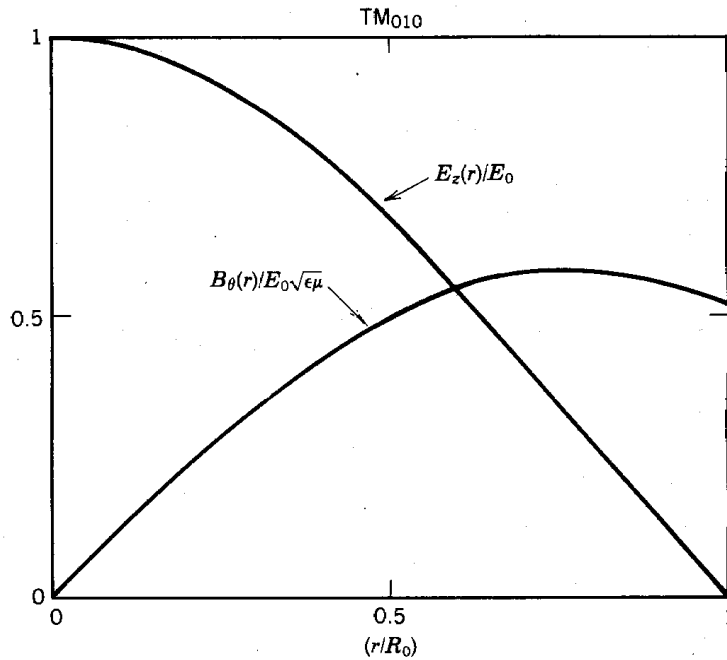


Figure 12.7 Normalized electric axial electric field and azimuthal magnetic field as a function of radius; TM_{010} mode in a cylindrical cavity.

Resonant Cavities and Waveguides

wavenumber k_n by

$$\omega_n = v k_n. \quad (12.44)$$

Angular frequency values are tabulated in Table 12.1.

The magnetic field of the modes can be calculated from Eq. (12.34),

$$\partial \mathbf{B} / \partial t = - (\nabla \times \mathbf{E}). \quad (12.45)$$

Magnetic field is directed along the θ direction. Assuming time variation $\exp(j\omega t)$ and substituting from Eq. (12.43),

$$j\omega_n B_{\theta n} = dE_{zn}/dr = E_{0n} dJ_0(k_n r)/dr. \quad (12.46)$$

Rewriting Eq. (12.46),

$$B_{\theta n}(r) = -j \sqrt{\epsilon\mu} E_{0n} J_1(k_n r).$$

Magnetic field variation for the TM_{010} mode is plotted in Figure 12.7. The magnetic field is zero on the axis. Moving outward in radius, B_θ increases linearly. It is proportional to the integral of axial displacement current from 0 to r . Toward the outer radius, there is little additional contribution of the displacement current. The $1/r$ factor [see Eq. (4.40)] dominates, and the magnitude of B_θ decreases toward the wall.

12.4 PROPERTIES OF THE CYLINDRICAL RESONANT CAVITY

In this section, we consider some of the physical implications of the solutions for resonant oscillations in a cylindrical cavity. The oscillations treated in the previous section are called TM_{0n0} modes. The term TM (transverse magnetic) indicates that magnetic fields are normal to the longitudinal direction. The other class of oscillations, TE modes, have longitudinal components of \mathbf{B} , and $E_z = 0$. The first number in the subscript is the azimuthal mode number; it is zero for azimuthally symmetric modes. The second number is the radial mode number. The radial mode number minus one is the number of nodes in the radial variation of E_z . The third number is the longitudinal mode number. It is zero in the example of Section 12.3 because E_z is constant in the z direction. The wavenumber and frequency of TM_{0n0} modes depends only on R_0 , not d . This is not generally true for other types of modes.

TM_{0n0} modes are optimal for particle acceleration. The longitudinal electric field is uniform along the propagation direction of the beam and its magnitude is maximum on axis. The

Resonant Cavities and Waveguides

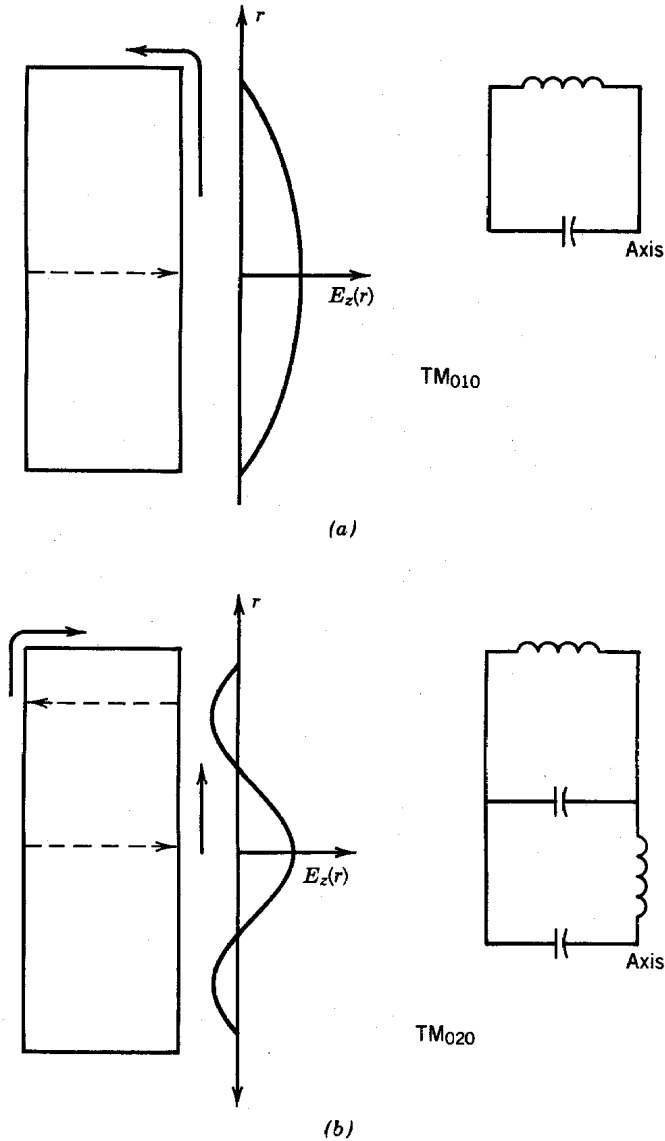


Figure 12.8 Spatial variations of axial electric field and equivalent circuits for electromagnetic oscillations in a cylindrical resonant cavity. Dashed line indicates displacement current, solid line indicates real current flow in the cavity walls. (a) TM_{010} mode. (b) TM_{020} mode.

transverse magnetic field is zero on axis; this is important for electron acceleration where transverse magnetic fields could deflect the beam. TM modes with nonzero longitudinal wavenumber ($p \neq 0$) have axial electric field of the form $E_z(0, z) \sim \sin(p\pi x/d)$; it is clear that the acceleration of particles crossing the cavity is reduced for these modes.

Figure 12.8 clarifies the nature of TM_{0n0} modes in terms of lumped circuit element approximations. Displacement currents and real currents are indicated along with equivalent circuit models. At values of n greater than 1, the cavity is divided into n interacting resonant LC

Resonant Cavities and Waveguides

circuits. The capacitance and inductance of each circuit is reduced by a factor of about $1/n$; therefore, the resonant frequency of the combination of elements is increased by a factor close to n .

Resonant cavities are usually constructed from copper or copper-plated steel for the highest conductivity. Nonetheless, effects of resistivity are significant because of the large reactive current. Resistive energy loss from the flow of real current in the walls is concentrated in the inductive regions of the cavity; hence, the circuit of Figure 12.3 is a good first-order model of an imperfect cavity. Current penetrates into the wall a distance equal to the skin depth [Eq. (10.7)]. Power loss is calculated with the assumption that the modes approximate those of an ideal cavity. The surface current per length on the walls is $J_s = B_\theta(r, z, t)/\mu_o$. Assuming that the current is distributed over a skin depth, power loss can be summed over the surface of the cavity. Power loss clearly depends on mode structure through the distribution of magnetic fields. The Q value for the TM_{010} mode of a cylindrical resonant cavity is

$$Q = \frac{d/\delta}{1 + d/R_0} \quad (12.48)$$

where the skin depth δ is a function of the frequency and wall material. In a copper cavity oscillating at $f = 1$ GHz, the skin depth is only $2 \mu\text{m}$. This means that the inner wall of the cavity must be carefully plated or polished; otherwise, current flow will be severely perturbed by surface irregularities lowering the cavity Q . With a skin depth of $2 \mu\text{m}$, Eq. (12.48) implies a Q value of 3×10^4 in a cylindrical resonant cavity of radius 12 cm and length 4 cm. This is a very high value compared to resonant circuits composed of lumped elements. Equation (12.32) implies that the bandwidth for exciting a resonance

$$\Delta f/f_0 \approx 1/Q = 3 \times 10^{-5}.$$

An rf power source that drives a resonant cavity must operate with very stable output frequency. For $f_0 = 1$ GHz, the allowed frequency drift is less than 33 kHz.

The total power lost to the cavity walls can be determined from Eq. (12.24) if the stored energy in the cavity, U , is known. The quantity can be calculated from Eq. (12.43) for the TM_{010} mode; we assume the calculation is performed at the time when magnetic fields are zero.

$$U = \int_0^d dz \int_0^{R_0} 2\pi r dr (\epsilon E_o^2/2) J_0^2(2.405r/R_0) = (\pi R_0^2 d) (\epsilon E_o^2/2) J_1^2(2.405). \quad (12.49)$$

A cylindrical cavity can support a variety of resonant modes, generally at higher frequency than the fundamental accelerating mode. Higher-order modes are generally undesirable. They do not

Resonant Cavities and Waveguides

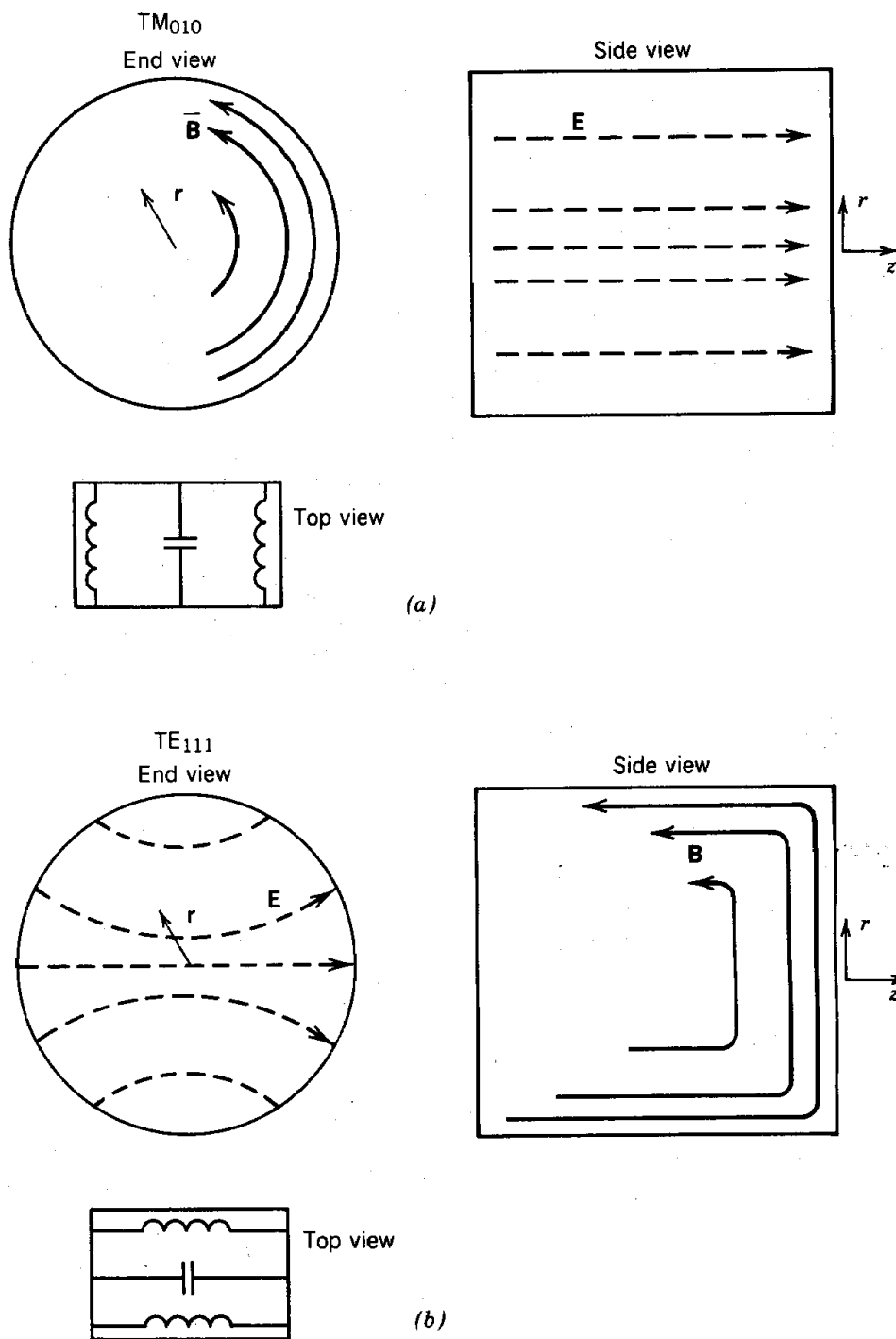


Figure 12.9 Field variations and distribution of capacitance and inductance in cylindrical resonant cavity. (a) TM_{010} mode. (b) TE_{111} mode.

Resonant Cavities and Waveguides

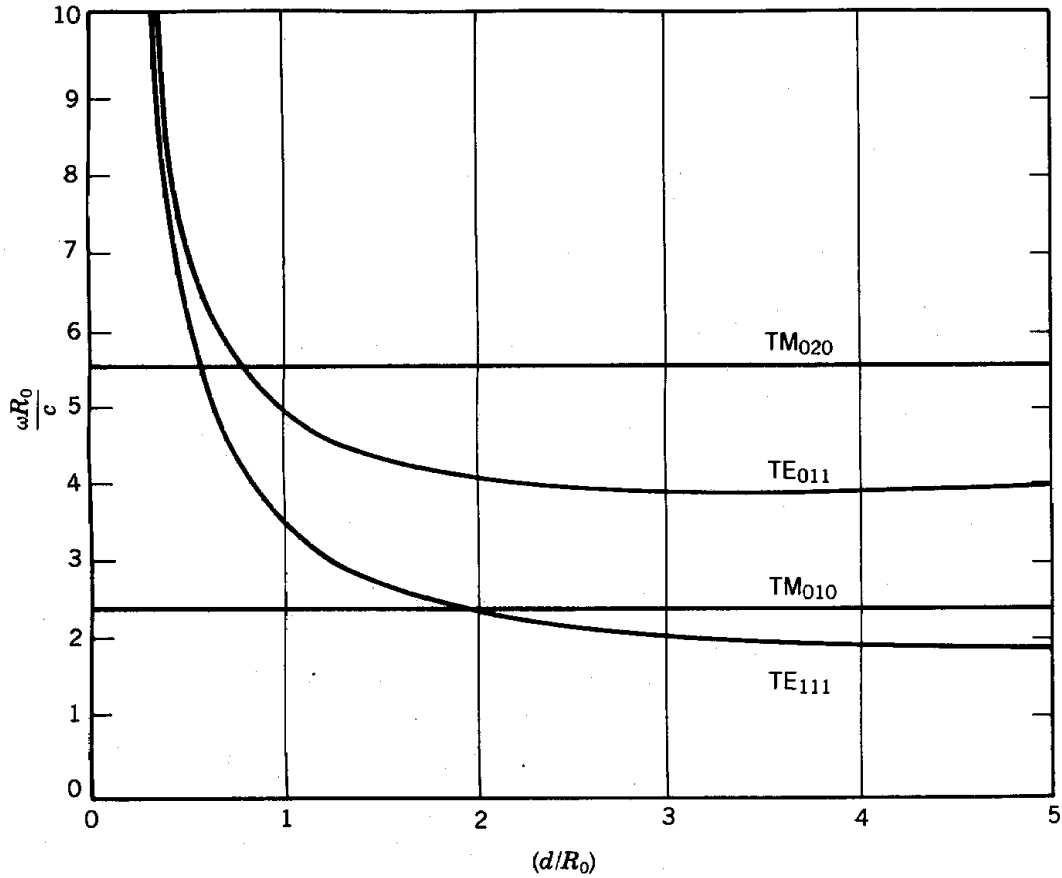


Figure 12.10 Variation of resonant angular frequency with geometry of cylindrical resonant cavity for various low-frequency modes.

contribute to particle acceleration; the energy shunted into higher-order modes is wasted. Sometimes, they interfere with particle acceleration; modes with transverse field components may induce beam deflections and particle losses.

As an example of an alternate mode, consider the lowest frequency TE mode, the TE_{111} mode. Figure 12.9 shows a sketch of the electric and magnetic fields. The displacement current oscillates from side to side across the diameter of the cavity. Magnetic fields are wrapped around the displacement current and have components in the axial direction. The distribution of capacitance and inductance for TE_{111} oscillations is also shown in Figure 12.9. The mode frequency depends on the cavity length (Fig. 12.10). As d increases over the range $d \ll R_0$ to $d \geq R_0$, there is a large increase in the capacitance of the cavity for displacement current flow across a diameter. Thus, the resonant frequency drops. For $d \gg R_0$, return current flows mainly back along the circular wall of the cavity. Therefore, the ratio of electric to magnetic field energy in the cavity approaches a constant value, independent of d . Inspection of Figure 2.10 shows that in long cavities, the TE_{111} mode has a lower frequency than the TM_{010} . Care must be taken not to excite the TE_{111} mode in parameter regions where there is *mode degeneracy*. The term degeneracy

indicates that two modes have the same resonant frequency. Mode selection is a major problem in the complex structures used in linear ion accelerators. Generally, the cavities are long cylinders with internal structures; the mode plot is considerably more complex than Figure 12.10. There is a greater possibility for mode degeneracy and power coupling between modes. In some cases, it is necessary to add metal structures to the cavity, which selectively damp competing modes.

12.5 POWER EXCHANGE WITH RESONANT CAVITIES

Power must be coupled into resonant cavities to maintain electromagnetic oscillations when there is resistive damping or a beam load. The topic of power coupling to resonant cavities involves detailed application of microwave theory. In this section, the approach is to achieve an understanding of basic power coupling processes by studying three simple examples.

We have already been introduced to a cavity with the power feed located on axis. The feed drives a beam and supplies energy lost to the cavity walls. In this case, power is electrically coupled to the cavity because the current in the power feeds interacts predominantly with electric fields. Although this geometry is never used for driving accelerator cavities, there is a practical application of the inverse process of driving cavity oscillations by a beam. Figure 12.11a shows a klystron, a microwave generator. An on-axis electron beam is injected across the cavity. The electron beam has time-varying current with a strong Fourier component at the resonant frequency of the cavity, ω_0 . We will consider only this component of the current and represent it as a harmonic current source. The cavity has a finite Q , resulting from wall resistance and extraction of microwave energy.

The complete circuit model for the TM_{010} mode is shown in Figure 12.11b. The impedance presented to the component of the driving beam current with frequency ω is

$$Z = (j\omega L + R) / [(1 - \omega^2 LC) + j\omega RC]. \quad (12.50)$$

Assuming that $\omega = \omega_0 - 1/\sqrt{LC}$ and that the cavity has high Q , Eq. (12.50) reduces to

$$Z \cong L/RC = Z_0^2/R = QZ_0, \quad (12.51)$$

with Q given by Eq. (12.27). The impedance is resistive; the voltage oscillation induced is in phase with the driving current so that energy extraction is maximized. Equation (12.51) shows that the cavity acts as a step-down transformer when the power feed is on axis. Power at low current and high voltage (impedance Z_0^2/R) drives a high current through resistance R .

In applications to high-energy accelerators, the aim is to use resonant cavities as step-up transformers. Ideally, power should be inserted at low impedance and coupled to a low-current

Resonant Cavities and Waveguides

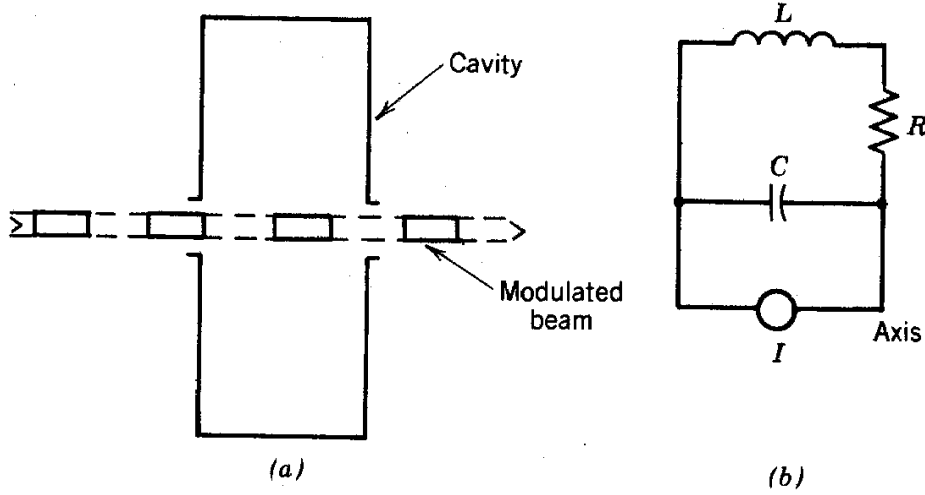


Figure 12.11 Electromagnetic oscillations in resonant cavity driven by modulated beam on axis (klystron). (a) Geometry. (b) Equivalent circuit.

beam at high voltage. This process is accomplished when energy is *magnetically coupled* into a cavity. With magnetic coupling, the power input is close to the outer radius of the cavity; therefore, interaction is predominantly through magnetic fields. A method for coupling energy to the TM_{010} mode is illustrated in Figure 12.12a. A loop is formed on the end of a transmission line. The loop is orientated to encircle the azimuthal magnetic flux of the TM_{010} mode. (A loop optimized to drive the TE_{111} mode would be rotated 90° to couple to radial magnetic fields.)

We shall first consider the inverse problem of extracting the energy of a TM_{010} oscillation through the loop. Assume that the loop couples only a small fraction of the cavity energy per oscillation period. In this case, the magnetic fields of the cavity are close to the unperturbed distribution. The magnetic field at the loop position, ρ , is

$$B(t) = B_0(\rho, t) \cos \omega t, \quad (12.52)$$

where $B_0(\rho, t)$ is a slowly varying function of time. The spatial variation is given by Eq. (12.47). The loop is attached to a transmission line that is terminated by a matched resistor R .

The voltage induced at the loop output depends on whether the loop current significantly affects the magnetic flux inside the loop. As we saw in the discussion of the Rogowski loop (Section 9.14), the magnetic field inside the loop is close to the applied field when $L/R \ll 1/\omega_o$, where L is the loop inductance and $1/\omega_o$ is the time scale for magnetic field variations. In this limit, the magnitude of the induced voltage around a loop of area A_l is $V \approx A_l \omega_o B_0$. The extracted power is

Resonant Cavities and Waveguides

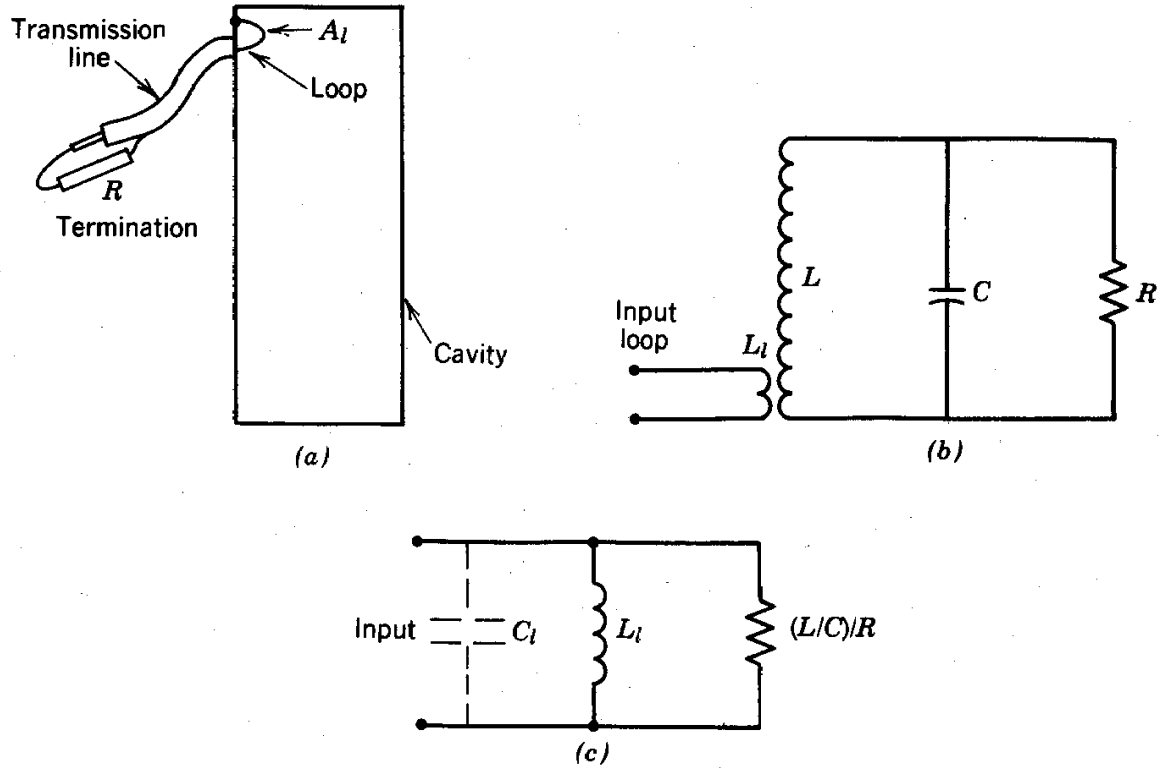


Figure 12.12 Resonant cavity interactions with magnetic coupling loop. (a) Geometry of loop set up to extract energy from cavity. (b) Equivalent circuit model to give input impedance of loop coupled to cavity. (c) Circuit of part b at resonance (transformer replaced by its equivalent circuit).

$$P \cong (A_l B_0 \omega)^2 / 2R. \quad (12.53)$$

Power coupled out of the cavity increases as A_l^2 in this regime. At the opposite extreme ($L/R \gg 1/\omega_o$), the loop voltage is shifted 90° in phase with respect to the magnetic field. Application of Eq. (9.124) shows that the extracted power is approximately

$$P \cong [A_l B_0 / (L/R)]^2 / 2R. \quad (12.54)$$

Because the loop inductance is proportional to A_l , the power is independent of the loop area in this limit. Increasing A_l increases perturbations of the cavity modes without increasing power output. The optimum size for the coupling loop corresponds to maximum power transfer with minimum perturbation, or $L/R \sim 1/\omega_o$.

Resonant Cavities and Waveguides

Note that in Eqs. (12.53) and (12.54), power loss from the cavity is proportional to B_0^2 and is therefore proportional to the stored energy in the cavity, U . The quantity U is governed by the equation

$$dU/dt \sim -U. \quad (12.55)$$

The stored energy decays exponentially; therefore, losses to the loop can be characterized by a Q factor Q_l . If there are also resistive losses in the cavity characterized by Q_c , then the total cavity Q is

$$Q = (1/Q_l + 1/Q_c)^{-1}. \quad (12.56)$$

We can now proceed to develop a simple circuit model to describe power transfer through a magnetically coupled loop into a cavity with a resistive load on axis. The treatment is based on our study of the transformer (Section 9.2). The equivalent circuit model is illustrated in Figure 12.12b. The quantity R represents the on-axis load. We consider the loop as the primary and the flow of current around the outside of the cavity as the secondary. The primary and secondary are linked together through shared magnetic flux. The loop area is much smaller than the cross-section area occupied by cavity magnetic fields. An alternate view of this situation is that there is a large secondary inductance, only part of which is linked to the primary.

Following the derivation of Section 9.2, we can construct the equivalent circuit seen from the primary input (Fig. 12.12c). The part of the cavity magnetic field enclosed in the loop is represented by L_l ; the secondary series inductance is $L - L_l$. We assume that energy transfer per oscillation period is small and that $L_l \ll L$. Therefore, the magnetic fields are close to those of an unperturbed cavity. This assumption allows a simple estimate of L_l .

To begin, we neglect the effect of the shunt inductance L_l in the circuit of Figure 12.12c and calculate the impedance the cavity presents at the loop input. The result is

$$Z = [j\omega L + R(1 - \omega^2 LC)] / (1 + j\omega RC). \quad (12.57)$$

Damping must be small for an oscillatory solution. This is true if the load resistance is high, or $R \gg \sqrt{LC}$. Assuming this limit and taking $\omega = \omega_0$, Eq. (12.57) becomes

$$Z \cong R [(L/C)/R^2]. \quad (12.58)$$

Equation (12.58) shows that the cavity presents a purely resistive load with impedance much smaller than R . The combination of coupling loop and cavity act as a step-up transformer.

We must still consider the effect of the primary inductance in the circuit of Figure 12.12c. The best match to typical power sources occurs when the total input impedance is resistive. A simple

Resonant Cavities and Waveguides

method of matching is to add a shunt capacitor C_1 , with a value chosen so that $C_1 L_1 = LC$. In this case, the parallel combination of L_1 and C_1 has infinite impedance at resonance, and the total load is $(L/C)/R$. Matching can also be performed by adjustment of the transmission line leading to the cavity. We shall see in Section 12.6 that transmission lines can act as impedance transformers. The total impedance will appear to be a pure resistance at the generator for input at a specific frequency if the generator is connected to the cavity through a transmission line of the proper length and characteristic impedance.

12.6 TRANSMISSION LINES IN THE FREQUENCY DOMAIN

In the treatment of the transmission line in Section 9.8, we considered propagating voltage pulses with arbitrary waveform. The pulses can be resolved into frequency components by Fourier analysis. If the waveform is limited to a single frequency, the description of electromagnetic signal propagation on a transmission line is considerably simplified. In complex exponential notation, current is proportional to voltage. The proportionality constant is a complex number, containing information on wave amplitude and phase. The advantage is that wave propagation problems can be solved algebraically, rather than through differential equations.

Voltage waveforms in a transmission line move at a velocity $v = 1/\sqrt{\epsilon\mu}$ along the line. A harmonic disturbance in a transmission line may have components that travel in the positive or negative directions. A single-frequency voltage oscillation measured by a stationary observer has the form

$$V(z,t) = V_+ \exp[j\omega(t-z/v)] + V_- \exp[j\omega(t+z/v)]. \quad (12.59)$$

Equation (12.59) states that points of constant V move along the line at speed v in either the positive or negative z directions. As we found in Section 9.9, the current associated with a wave traveling in either the positive or negative direction is proportional to the voltage. The constant of proportionality is a real number, Z_0 . The total current associated with the voltage disturbance of Eq. (12.59) is

$$I(z,t) = (V_+/Z_0) \exp[j\omega(t-z/v)] - (V_-/Z_0) \exp[j\omega(t+z/v)]. \quad (12.60)$$

Note the minus sign in the second term of Eq. (12.60). It is included to preserve the convention that current is positive when positive waves move in the $+z$ direction. A voltage wave with positive voltage moving in the $-z$ direction has negative current. The total impedance at a point is, by definition

$$Z = V(z,t)/I(z,t). \quad (12.61)$$

Resonant Cavities and Waveguides

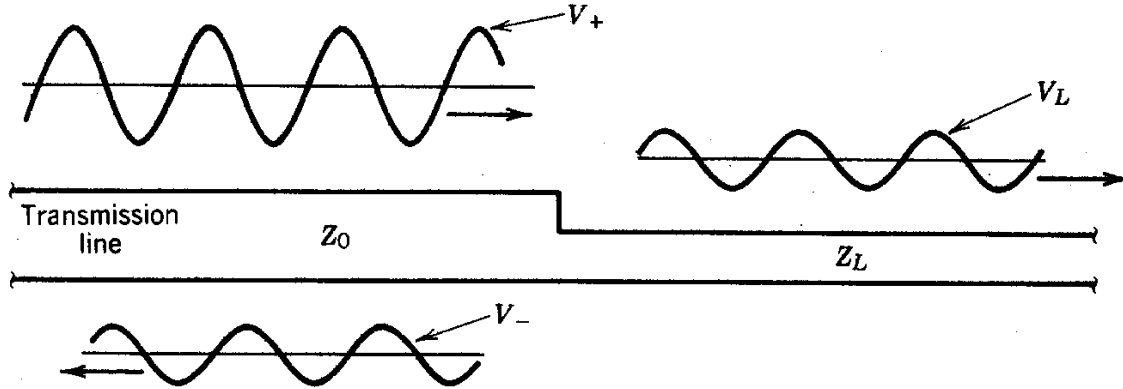


Figure 12.13 Incident, transmitted, and reflected waves at junction of two transmission lines.

If there are components of $V(z, t)$ moving in both the positive and negative directions, Z may not be a real number. Phase differences arise because the sum of V_+ and V_- may not be in phase with the sum of I_+ and I_- .

We will illustrate transmission line properties in the frequency-domain by the calculation of wave reflections at a discontinuity. The geometry is illustrated in Figure 12.13. Two infinite length transmission lines are connected at $z = 0$. Voltage waves at angular ω frequency travel down the line with characteristic impedance Z_0 toward the line with impedance Z_L . If $Z_L = Z_0$, the waves travel onward with no change and disappear down the second line. If $Z_L \neq Z_0$, we must consider the possibility that wave reflections take place at the discontinuity. In this case, three wave components must be included:

1. The incident voltage wave, of form $V_+ \exp[j\omega(t-z/v)]$ is specified. The current of the wave is $(V_+/Z_0) \exp[j\omega(t-z/v)]$.
2. Some of the incident wave energy may continue through the connection into the second line. The wave moves in the $+z$ direction and is represented by $V_L \exp[j\omega(t-z/v)]$. The current of the *transmitted* wave is $(V_L/Z_L) \exp[j\omega(t-z/v)]$. There is no negatively directed wave in the second line because the line has infinite length.
3. Some wave energy may be reflected at the connection, leading to a backward-directed wave in the first line. The voltage and current of the reflected wave are $V_- \exp[j\omega(t-z/v)]$ and $-(V_-/Z_0) \exp[j\omega(t-z/v)]$.

The magnitudes of the transmitted and reflected waves are related to the incident wave and the properties of the lines by applying the following conditions at the connection point ($z = 0$):

Resonant Cavities and Waveguides

1. The voltage in the first line must equal the voltage in the second line at the connection.
2. All charge that flows into the connection must flow out.

The two conditions can be expressed mathematically in terms of the incident, transmitted, and reflected waves.

$$V_+ \exp(j\omega t) + V_- \exp(j\omega t) = V_L \exp(j\omega t), \quad (12.62)$$

$$(V_+/Z_o) \exp(j\omega t) - (V_-/Z_o) \exp(j\omega t) = (V_L/Z_L) \exp(j\omega t). \quad (12.63)$$

Canceling the time dependence, Eqs. (12.62) and (12.63) can be solved to relate the reflected and transmitted voltages to the incident voltage:

$$\rho = (V_-/V_+) = (Z_L - Z_o)/(Z_L + Z_o), \quad (12.64)$$

$$\tau = (V_L/V_+) = 2Z_o/(Z_L + Z_o). \quad (12.65)$$

Equations (12.64) and (12.65) define the reflection coefficient ρ and the transmission coefficient τ . The results are independent of frequency; therefore, they apply to transmission and reflection of voltage pulses with many frequency components. Finally, Eqs. (12.64) and (12.65) also hold for reflection and absorption of waves at a resistive termination, because an infinite length transmission line is indistinguishable from a resistor with $R = Z_L$.

A short-circuit termination has $Z_L = 0$. In this case, $\rho = -1$ and $\tau = 0$. The wave is reflected with inverted polarity, in agreement with Section 9.10. There is no transmitted wave. When $Z_L \Rightarrow \infty$ there is again no transmitted wave and the reflected wave has the same voltage as the incident wave. Finally, if $Z_L = Z_o$, there is no reflected wave and $\tau = 1$; the lines are matched.

As a final topic, we consider transformations of impedance along a transmission line. As shown in Figure 12.14, assume there is a load Z_L at $z = 0$ at the end of a transmission line of length l and characteristic impedance Z_o . The load may consist of any combination of resistors, inductors, and capacitors; therefore, Z_L may be a complex number. A power source, located at the point $z = -l$ produces a harmonic input voltage, $V_o \exp(j\omega t)$. The goal is to determine how much current the source must supply in order to support the input voltage. This is equivalent to calculating the impedance $Z(-l)$.

The impedance at the generator is generally different from Z_L . In this sense, the transmission line is an *impedance transformer*. This property is useful for matching power generators to loads that contain reactive elements. In this section, we shall find a mathematical expression for the transformed impedance. In the next section, we shall investigate some of the implications of the result.

Resonant Cavities and Waveguides

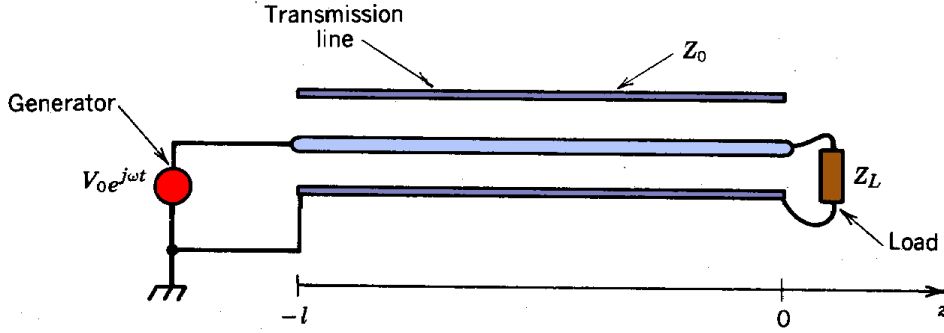


Figure 12.14 Connection of ac voltage generator to a load through transmission line.

Voltage waves are represented as in Eq. (12.59). Both a positive wave traveling from the generator to the load and a reflected wave must be included. All time variations have the form $\exp(j\omega t)$. Factoring out the time dependence, the voltage and current at $z = 0$ are

$$V(0) = V_+ + V_-, \quad (12.66)$$

$$I(0) = (V_+/Z_0) - (V_-/Z_0). \quad (12.67)$$

The voltage and current at $z = -l$ are

$$V(-l) = V_+ \exp(+jl\omega/v) + V_- \exp(-jl\omega/v), \quad (12.68)$$

$$I(-l) = (V_+/Z_0) \exp(+jl\omega/v) - (V_-/Z_0) \exp(-jl\omega/v). \quad (12.69)$$

Furthermore, the treatment of reflections at a line termination [Eq. (12.64)] implies that

$$V_-/V_+ = (Z_L - Z_0)/(Z_L + Z_0). \quad (12.70)$$

Taking $Z(-l) = V(-l)/I(-l)$, and substituting from q. (12.70), we find that

$$\begin{aligned} Z(-l) &= Z_0 \frac{\exp(jl\omega/v) + (Z_L - Z_0)\exp(-l\omega/v)/(Z_L + Z_0)}{\exp(jl\omega/v) - (Z_L - Z_0)\exp(-l\omega/v)/(Z_L + Z_0)} \\ &= Z_0 \frac{Z_L[\exp(jl\omega/v) + \exp(-jl\omega/v)] + Z_0[\exp(jl\omega/v) - \exp(-jl\omega/v)]}{Z_L[\exp(jl\omega/v) - \exp(-jl\omega/v)] + Z_0[\exp(jl\omega/v) + \exp(-jl\omega/v)]} \\ &= Z_0 \frac{Z_L \cos(2\pi l/\lambda) + jZ_0 \sin(2\pi l/\lambda)}{Z_0 \cos(2\pi l/\lambda) + jZ_L \sin(2\pi l/\lambda)}. \end{aligned} \quad (12.71)$$

Resonant Cavities and Waveguides

where $\omega/v = 2\pi/\lambda$. In summary, the expressions of Eq. (12.71) give the impedance at the input of a transmission line of length l terminated by a load Z_L .

12.7 TRANSMISSION LINE TREATMENT OF THE RESONANT CAVITY

In this section, the formula for the transformation of impedance by a transmission line [Eq. (12.71)] is applied to problems related to resonant cavities. To begin, consider terminations at the end of a transmission line with characteristic impedance Z_o and length l . The termination Z_L is located at $z = 0$ and the voltage generator at $z = -l$. If Z_L is a resistor with $R = Z_o$, Eq. (12.71) reduces to $Z(-l) = Z_o$, independent of the length of the line. In this case, there is no reflected wave. The important property of the matched transmission line is that the voltage wave at the termination is identical to the input voltage wave delayed by time interval l/v . Matched lines are used to conduct diagnostic signals without distortion.

Another interesting case is the short-circuit termination, $Z_L = 0$. The impedance at the line input is

$$Z(-l) = jZ_o \tan(2\pi l/\lambda). \quad (12.72)$$

The input impedance is zero when $l = 0, \lambda/2, 3\lambda/2, \dots$. An interesting result is that the shorted line has infinite input impedance (open circuit) when

$$l = \lambda/4, 3\lambda/4, 5\lambda/4, \dots \quad (12.73)$$

A line with length given by Eq. (12.73) is called a *quarter wave line*.

Figure 12.15 illustrates the analogy between a cylindrical resonant cavity and a quarter wave line. A shorted radial transmission line of length l has power input at frequency ω at the inner diameter. Power flow is similar to that of Figure 12.2. If the frequency of the input power matches one of the resonant frequencies of the line, then the line has an infinite impedance and power is transferred completely to the load on axis. The resonant frequencies of the radial transmission line are

$$\omega_1 = \pi v/2l, \quad \omega_2 = 3\pi v/2l, \quad \omega_3 = 5\pi v/2l, \dots \quad (12.74)$$

These frequencies differ somewhat from those of Table 12.1 because of geometric differences between the cavities.

The quarter wave line has positive and negative-going waves. The positive wave reflects at the short-circuit termination giving a negative-going wave with 180° phase shift. The voltages of the waves subtract at the termination and add at the input ($z = -l$). The summation of the voltage waves is a standing-wave pattern:

Resonant Cavities and Waveguides

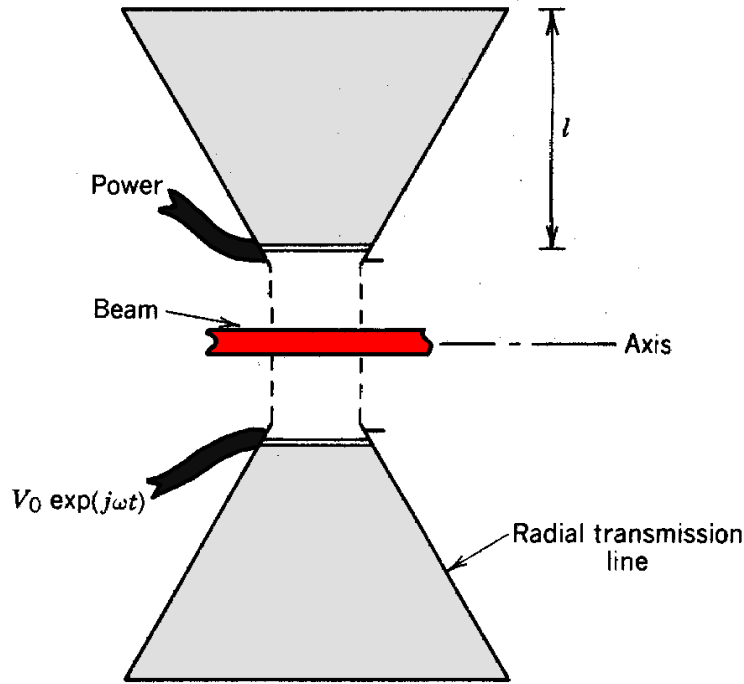


Figure 12.15 Resonant acceleration cavity formed from shorted radial transmission line.

$$V(z,t) = V_0 \sin(-\pi z/2l) \exp(j\omega t).$$

At resonance, the current of the two waves at $z = l$ is equal and opposite. The line draws no current and has infinite impedance. At angular frequencies below ω_1 , inspection of Eq. (12.72) shows that $Z \sim +j$; thus, the shorted transmission line acts like an inductor. For frequencies above ω_1 , the line has $Z \sim -j$; it acts as a capacitive load. This behavior repeats cyclically about higher resonant frequencies.

A common application of transmission lines is power matching from a harmonic voltage generator to a load containing reactive elements. We have already studied one example of power matching, coupling of energy into a resonant cavity by a magnetic loop (Section 12.5). Another example is illustrated in Figure 12.16. An ac generator drives an acceleration gap. Assume, for simplicity, that the beam load is modeled as a resistor R . The generator efficiency is optimized when the total load is resistive. If the load has reactive components, the generator must supply displacement currents that lead to internal power dissipation. Reactances have significant effects at high frequency. For instance, displacement current is transported through the capacitance between the electrodes of the accelerating gaps, C_g . The displacement current is comparable to the load current when $\omega \sim 1/RC_g$. In principle, it is unnecessary for the power supply to support displacement currents because energy is not absorbed by reactances. The strategy is to add circuit elements that can support the reactive current, leaving the generator to supply power only to the

Resonant Cavities and Waveguides

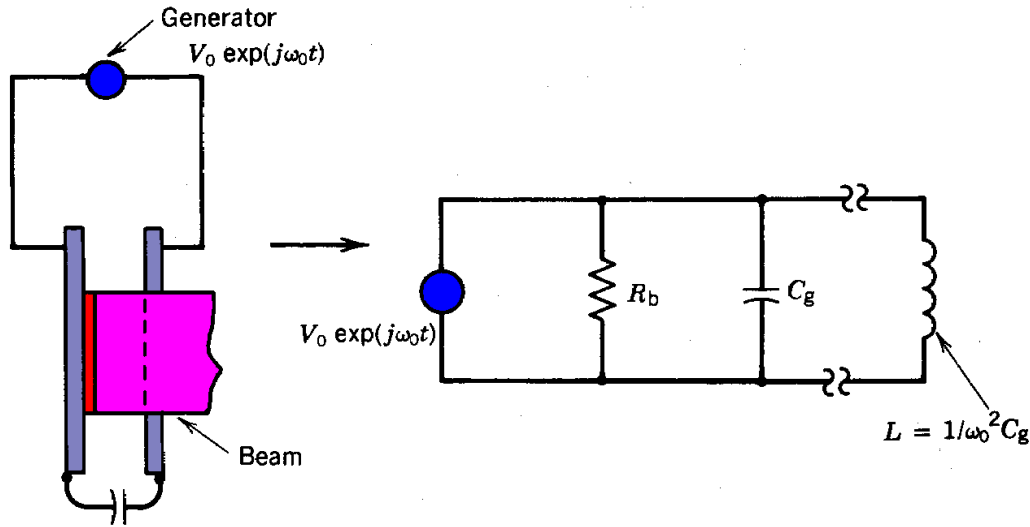


Figure 12.16 Power matching of harmonic generators to loads with reactive and resistive components. Geometry and equivalent circuit of acceleration gap at high frequency.

resistive load. This is accomplished in the acceleration gap by adding a shunt inductance with value $L = 1/\omega_o^2 C_g$, where ω_o is the generator frequency. The improvement of the Wideroe linac by the addition of resonant cavities (Section 14.2) is an example of this type of matching.

Section 12.5 shows that a coupling loop in a resonant cavity is a resistive load at the driving frequency if the proper shunt capacitance is added. Matching can also be accomplished by adjusting the length of the transmission line connecting the generator to the loop. At certain values of line length, the reactances of the transmission line act in concert with the reactances of the loop to support displacement current internally. The procedure for finding the correct length consists of adjusting parameters in Eq. (12.71) with Z_1 equal to the loop impedance until the imaginary part of the right-hand side is equal to zero. In this circumstance, the generator sees a purely resistive load. The search for a match is aided by use of the Smith chart; the procedure is reviewed in most texts on microwaves.

12.8 WAVEGUIDES

Resonant cavities have finite extent in the axial direction. Electromagnetic waves are reflected at the axial boundaries, giving rise to the standing-wave patterns that constitute resonant modes. We shall remove the boundaries in this section and study electromagnetic oscillations that travel in the axial direction. A structure that contains a propagating electromagnetic wave is called a *waveguide*. Consideration is limited to metal structures with uniform cross section and infinite extent in the z direction. In particular, we will concentrate on the cylindrical waveguide, which is simply a hollow tube.

Resonant Cavities and Waveguides

Waveguides transport electromagnetic energy. Waveguides are often used in accelerators to couple power from a microwave source to resonant cavities. Furthermore, it is possible to transport particle beams in a waveguide in synchronism with the wave phase velocity so that they continually gain energy. Waveguides used for direct particle acceleration must support slow waves with phase velocity equal to or less than the speed of light. Slow-wave structures have complex boundaries that vary periodically in the axial direction; the treatment of slow waves is deferred to Section 12.9.

Single-frequency waves in a guide have fields of the form $\exp[j(\omega t - kz)]$ or $\exp[j(\omega t + kz)]$. Electromagnetic oscillations move along the waveguide at velocity ω/k . In contrast to transmission lines, waveguides do not have a center conductor. This difference influences the nature of propagating waves in the following ways:

1. The phase velocity in a waveguide varies with frequency. A structure with frequency-dependent phase velocity exhibits *dispersion*. Propagation in transmission lines is dispersionless.
2. Waves of any frequency can propagate in a transmission line. In contrast, low-frequency waves cannot propagate in a waveguide. The limiting frequency is called the *cutoff frequency*.
3. The phase velocity of waves in a waveguide is greater than the speed of light. This does not violate the principles of relativity since information can be carried only by modulation of wave amplitude or frequency. The propagation velocity of frequency modulations is the group velocity, which is always less than the speed of light in a waveguide.

The properties of waveguides are easily demonstrated by a lumped circuit element analogy. We can generate a circuit model for a waveguide by starting from the transmission line model introduced in Section 9.9. A coaxial transmission line is illustrated in Figure 12.17a. At frequencies low compared to $1/(R_o - R_i)\sqrt{\epsilon\mu}$, the field pattern is the familiar one with radial electric fields and azimuthal magnetic fields. This field is a TEM (transverse electric and magnetic) mode; both the electric and magnetic fields are transverse to the direction of propagation. Longitudinal current is purely real, carried by the center conductor. Displacement current flows radially; longitudinal voltage differences result from inductive fields. The equivalent circuit model for a section of line is shown in Figure 12.17a.

The field pattern may be modified when the radius of the center conductor is reduced and the frequency is increased. Consider the limit where the wavelength of the electromagnetic disturbance, $\lambda = 2\pi/k$, is comparable to or less than the outer radius of the line. In this case, voltage varies along the high-inductance center conductor on a length scale $\leq R_o$. Electric field lines may directly connect regions along the outer conductor (Fig. 12.17b). The field pattern is no longer a TEM mode because there are longitudinal components of electric field. Furthermore, a portion of the longitudinal current flow in the transmission line is carried by displacement current. An equivalent circuit model for the coaxial transmission line at high frequency is shown in Figure

Resonant Cavities and Waveguides

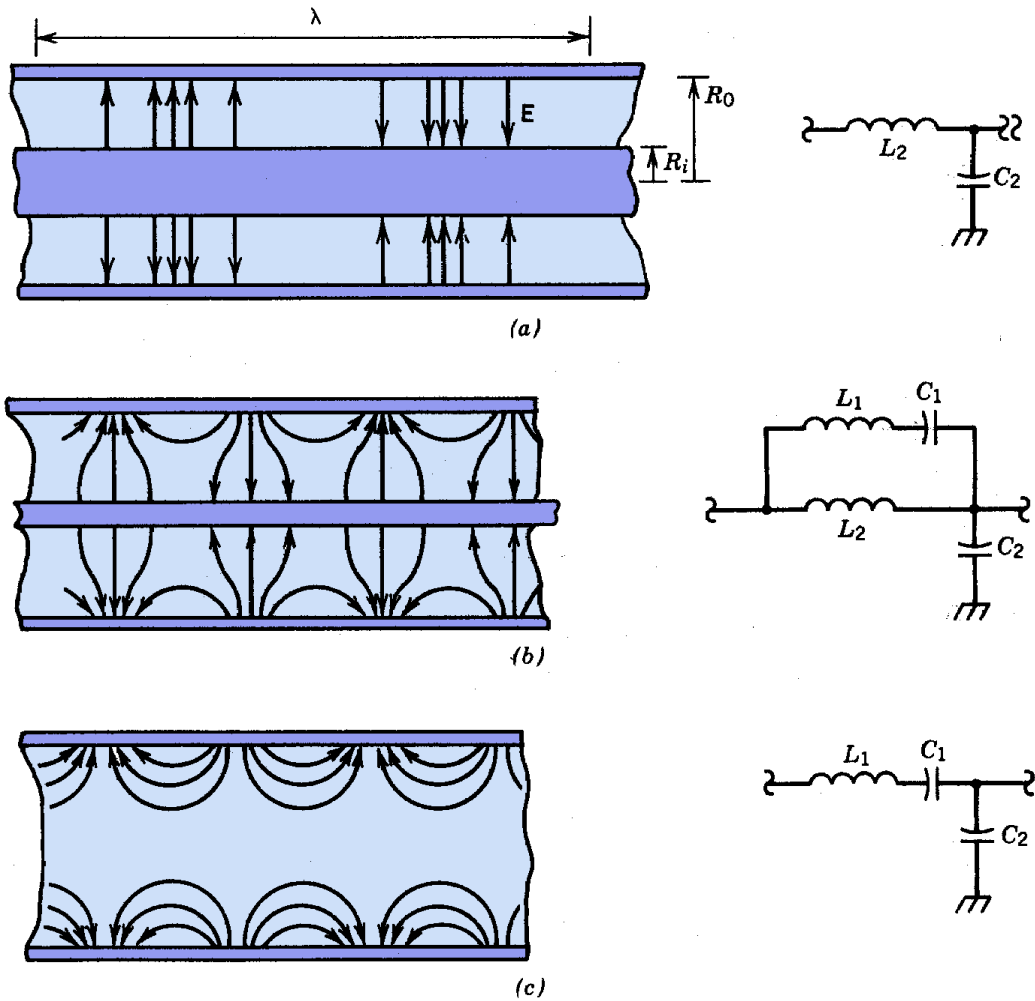


Figure 12.17 Propagating waves in coaxial transmission lines and circular waveguides, electric field patterns, and equivalent circuits. (a) TEM mode in transmission line, low frequency. (b) TM mode in transmission line, high frequency. (c) TM_{10} mode in waveguide.

12.17b. The capacitance between the inner and outer conductors, C_2 , is reduced. The flow of real current through inductor L_2 is supplemented by axial displacement current through the series combination of C_1 and L_1 . The inductance L_1 is included because displacement currents generate magnetic fields.

As the diameter of the center conductor is reduced, increasing L_2 , a greater fraction of the axial current is carried by displacement current. The limit where $R_i \Rightarrow 0$ is illustrated in Figure 12.17c. All axial current flow is via displacement current; L_2 is removed from the mode. The field pattern and equivalent circuit model are shown. We can use the impedance formalism to find the appropriate wave equations for the circuit of Figure 12.17c. Assume that there is a wave moving in the $+z$ direction and take variations of voltage and current as

Resonant Cavities and Waveguides

$$V = V_+ \exp[j(\omega t - kz)] \quad \text{and} \quad I = I_+ \exp[j(\omega t - kz)].$$

The waveguide is separated into sections of length Δz . The inductance of a section is $l_1 \Delta z$ where l_1 is the inductance per unit length. The quantity C_2 equals $c_2 \Delta z$, where c_2 is the shunt capacitance per unit length in farads per meter. The series capacitance is inversely proportional to length, so that $C_1 = c_1 \Delta z$, where c_1 is the series capacitance of a unit length. The quantity c_1 has units of farad-meters. The voltage drop across an element is the impedance of the element multiplied by the current or

$$\Delta V = -I (-j\Delta z/\omega c_1 + j\omega l_1 \Delta z),$$

or

$$\partial V / \partial z = -(-j/\omega c_1 + j\omega l_1) I \quad (12.76)$$

The change in longitudinal current occurring over an element is equal to the current that is lost through C_2 to ground

$$\Delta I = -j c_2 \Delta z \omega V,$$

or

$$\partial I / \partial z = -j \omega c_2 V. \quad (12.77)$$

Equations (12.76) and (12.77) can be combined to the single-wave equation

$$\partial^2 V / \partial z^2 = -k^2 V = j \omega c_2 (-j/\omega c_1 + j\omega l_1) V = (c_2/c_1 - \omega^2 l_1 c_2) V. \quad (12.78)$$

Solving for k and letting $\omega_c = 1/\sqrt{l_1 c_1}$, we find that

$$k = \sqrt{c_2/c_1} \sqrt{\omega^2/\omega_c^2 - 1}. \quad (12.79)$$

Equation (12.79) relates the wavelength of the electromagnetic disturbance in the cylindrical waveguide to the frequency of the waves. Equation (12.79) is a dispersion relationship. It determines the phase velocity of waves in the guide as a function of frequency:

$$\omega/k = \sqrt{c_1/c_2} \omega_c / \sqrt{1 - \omega_c^2/\omega^2}.$$

Resonant Cavities and Waveguides

Note that the phase velocity is dispersive. It is minimum at high frequency and approaches infinity as $\omega \rightarrow \omega_c$. Furthermore, there is a *cutoff frequency*, ω_c , below which waves cannot propagate. The wavenumber is imaginary below ω_c . This implies that the amplitude of low-frequency waves decreases along the guide. Low-frequency waves are reflected near the input of the waveguide; the waveguide appears to be a short circuit.

The above circuit model applies to a propagating wave in the TM_{01} mode. The term TM refers to the fact that magnetic fields are transverse; only electric fields have a longitudinal component. The leading zero indicates that there is azimuthal symmetry; the 1 indicates that the mode has the simplest possible radial variation of fields. There are an infinite number of higher-order modes that can occur in a cylindrical transmission line. We will concentrate on the TM_{01} mode because it has the optimum field variations for particle acceleration. The mathematical methods can easily be extended to other modes. We will now calculate properties of azimuthally symmetric modes in a cylindrical waveguide by direct solution of the field equations. Again, we seek propagating disturbances of the form

$$\mathbf{E}(r, \theta, z, t) = \mathbf{E}(r, \theta) \exp[j(\omega t - kz)], \quad (12.80)$$

$$\mathbf{B}(r, \theta, z, t) = \mathbf{B}(r, \theta) \exp[j(\omega t - kz)]. \quad (12.81)$$

With the above variation and the condition that there are no free charges or current in the waveguide, the Maxwell equations [Eqs. (3.11) and (3.12)] are

$$\nabla \times \mathbf{E} = -j\omega \mathbf{B}, \quad (12.82)$$

$$\nabla \times \mathbf{B} = -j\omega \epsilon \mu \mathbf{E}. \quad (12.83)$$

Equations (12.82) and (12.83) can be combined to give the two wave equations

$$\nabla^2 \mathbf{E} = -k_o^2 \mathbf{E}, \quad (12.84)$$

$$\nabla^2 \mathbf{B} = -k_o^2 \mathbf{B}. \quad (12.85)$$

where $k_o = \sqrt{\epsilon \mu} \omega = \omega/v$.

The quantity k_o is the *free-space wavenumber*; it is equal to $2\pi/\lambda_o$, where λ_o is the wavelength of electromagnetic waves in the filling medium of the waveguide in the absence of the boundaries.

In principle, either Eq. (12.84) or (12.85) could be solved for the three components of \mathbf{E} or \mathbf{B} , and then the corresponding components of \mathbf{B} or \mathbf{E} found through Eq. (12.82) or (12.83). The process is complicated by the boundary conditions that must be satisfied at the wall radius, R_o :

Resonant Cavities and Waveguides

$$E_{\parallel}(R_o) = 0, \quad (12.86)$$

$$B_{\perp}(R_o) = 0. \quad (12.87)$$

Equations (12.86) and (12.87) refer to the vector sum of components; the boundary conditions couple the equations for different components. An organized approach is necessary to make the calculation tractable.

We will treat only solutions with azimuthal symmetry. Setting $\partial/\partial\theta = 0$, the component forms of Eqs. (12.82) and (12.83) are

$$jkE_{\theta} = -j\omega B_r, \quad (12.88)$$

$$(1/r) \partial(rE_{\theta})/\partial r = -j\omega B_z, \quad (12.89)$$

$$-jkE_r - \partial E_z/\partial r = -j\omega B_{\theta}, \quad (12.90)$$

$$jkB_{\theta} = -j(k_o^2/\omega) E_r, \quad (12.91)$$

$$(1/r) \partial(rB_{\theta})/\partial r = -j(k_o^2/\omega) E_z, \quad (12.92)$$

$$-jkB_r - \partial B_z/\partial r = -j(k_o^2/\omega) E_{\theta}. \quad (12.93)$$

These equations can be manipulated algebraically so that the transverse fields are proportional to derivatives of the longitudinal components:

$$B_r = -jk (\partial B_z/\partial r) / (k_o^2 - k^2), \quad (12.94)$$

$$E_r = -jk (\partial E_z/\partial r) / (k_o^2 - k^2), \quad (12.95)$$

$$B_{\theta} = -j(k^2/\omega) (\partial E_z/\partial r) / (k_o^2 - k^2), \quad (12.96)$$

$$E_{\theta} = -j\omega (\partial B_z/\partial r) / (k_o^2 - k^2). \quad (12.97)$$

Notice that there is no solution if both B_z and E_z equal zero; a waveguide cannot support a TEM mode. Equations (12.94)-(12.97) suggest a method to simplify the boundary conditions on the wave equations. Solutions are divided into two categories: waves that have $E_z = 0$ and waves that have $B_z = 0$. The first type is called a TE wave, and the second type is called a TM wave. The first type has transverse field components B_r and E_{θ} . The only component of magnetic field perpendicular to the metal wall is B_r . Setting $B_r = 0$ at the wall implies the simple, decoupled

Resonant Cavities and Waveguides

boundary condition

$$\partial B_z(R_o)/\partial r = 0. \quad (12.98)$$

Equation (12.98) implies that $E_\theta(R_o) = 0$ and $B_r(R_o) = 0$. The wave equation for the axial component of \mathbf{B} [Eq. (12.85)] can be solved easily with the above boundary condition. Given B_z , the other field components can be calculated from Eqs. (12.94) and (12.97).

For TM modes, the transverse field components are E_r and B_θ . The only component of electric field parallel to the wall is E_z so that the boundary condition is

$$E_z(R_o) = 0. \quad (12.99)$$

Equation (12.84) can be used to find E_z ; then the transverse field components are determined from Eqs. (12.95) and (12.96). The solutions for TE and TM waves are independent. Therefore, any solution with both E_z and B_z can be generated as a linear combination of TE and TM waves. The wave equation for E_z of a TM mode is

$$\nabla^2 E_z = (1/r) (\partial/\partial r) (\partial E_z/\partial r) - k_o^2 E_z = -k_o^2 E_z, \quad (12.100)$$

with $E_z(R_o) = 0$. The longitudinal contribution to the Laplacian follows from the assumed form of the propagating wave solution. Equation (12.100) is a special form of the Bessel equation. The solution is

$$E_z(r,z,t) = E_o J_0(\sqrt{k_o^2 - k^2} r) \exp[j(\omega t - kz)] \quad (12.101)$$

The boundary condition of Eq. (12.99) constraints the wavenumber in terms of the free-space wavenumber:

$$k_o^2 - k^2 = x_n^2/R_o^2, \quad (12.102)$$

where $x_n = 2.405, 5.520, \dots$. Equation (12.102) yields the following dispersion relationship for TM_{0n} modes in a cylindrical waveguide:

$$k = \sqrt{\epsilon\mu\omega^2 - x_n^2/R_o^2}, \quad (12.103)$$

The mathematical solution has a number of physical implications. First, the wavenumber of low-frequency waves is imaginary so there is no propagation. The cutoff frequency of the TM_{01} mode is

Resonant Cavities and Waveguides

$$\omega_c = 2.405/\sqrt{\epsilon\mu}R_o. \quad (12.104)$$

Near cutoff, the wavelength in the guide approaches infinity. The free-space wavelength of a TM_{01} electromagnetic wave at frequency ω_c is $\lambda_o \cong 2.61R_o$. The free-space wavelength is about equal to the waveguide diameter; waves with longer wavelengths are shorted out by the metal waveguide walls.

The wavelength in the guide is

$$\lambda = \lambda_o / \sqrt{1 - \omega_c^2/\omega^2}. \quad (12.105)$$

The phase velocity is

$$\omega/k = 1 / \sqrt{\epsilon\mu} \sqrt{1 - \omega_c^2/\omega^2}. \quad (12.106)$$

Note that the phase velocity in a vacuum waveguide is always greater than the speed of light.

The solution of the field equations indicates that there are higher-order TM_{0n} waves. The cutoff frequency for these modes is higher. In the frequency range $2.405/\sqrt{\epsilon\mu}R_o$ to $5.520/\sqrt{\epsilon\mu}R_o$, the only TM mode that can propagate is the TM_{01} mode. On the other hand, a complete solution for all modes shows that the TE_{11} has the cutoff frequency $\omega_c = 1.841/\sqrt{\epsilon\mu}R_o$ which is lower than that of the TM_{01} mode. Precautions must be taken not to excite the TE_{11} mode because: 1) the waves consume rf power without contributing to particle acceleration and 2) the on-axis radial electric and magnetic field components can cause deflections of the charged particle beam.

12.9 SLOW-WAVE STRUCTURES

The guided waves discussed in Section 12.8 cannot be used for particle acceleration because they have phase velocity greater than c . It is necessary to generate slow waves with phase velocity less than c . It is easy to show that slow waves cannot propagate in waveguides with simple boundaries. Consider, for instance, waves with electric field of the form $\exp[j(\omega t - kz)]$ with $\omega/k < c$ in a uniform cylindrical pipe of radius R_o . Because the wave velocity is assumed less than the speed of light, we can make a transformation to a frame moving at speed $u_z = \omega/k$. In this frame, the wall is unchanged and the wave appears to stand still. In the wave rest frame the electric field is static. Because there are no displacement currents, there is no magnetic field. The electrostatic field must be derivable from a potential. This is not consistent with the fact that the wave is surrounded by a metal pipe at constant potential. The only possible static field solution inside the pipe is $\mathbf{E} = 0$.

Slow waves can propagate when the waveguide has periodic boundaries. The properties of slow

Resonant Cavities and Waveguides

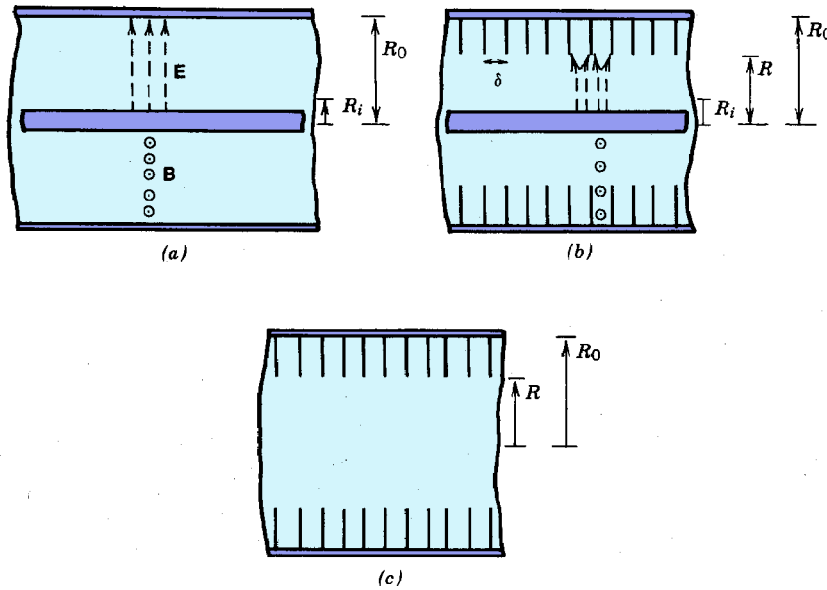


Figure 12.18 Slow-wave structures. (a) Electric and magnetic fields of TEM mode in coaxial transmission line. (b) Modified TEM mode in coaxial transmission line with capacitive loading. (c) Iris-loaded waveguide.

waves can be derived by a formal mathematical treatment of wave solutions in a periodic structure. In this section, we shall take a more physical approach, examining some special cases to understand how periodic structures support the boundary conditions consistent with slow waves. To begin, we consider the effects of the addition of periodic structures to the transmission line of Figure 12.18a. If the region between electrodes is a vacuum, TEM waves propagate with $\omega/k = c$. The line has a capacitance C and inductance L per unit length given by Eqs. (9.71) and (9.72). We found in Section 9.8 that the phase velocity of waves in a transmission line is related to these quantities by

$$\omega/k = 1/\sqrt{LC}. \quad (12.107)$$

Consider reconstructing the line as shown in Figure 12.18b. Annular metal pieces called *irises* are attached to the outer conductor. The irises have inner radius R and spacing δ .

The electric field patterns for a TEM wave are sketched in Figure 12.18b in the limit that the wavelength is long compared to δ . The magnetic fields are almost identical to those of the standard transmission line except for field exclusion from the irises; this effect is small if the irises are thin. In contrast, radial electric fields cannot penetrate into the region between irises. The electric fields are restricted to the region between the inner conductor and inner radius of the irises. The result is that the inductance per unit length is almost unchanged, but C is significantly increased. The capacitance per unit length is approximately

Resonant Cavities and Waveguides

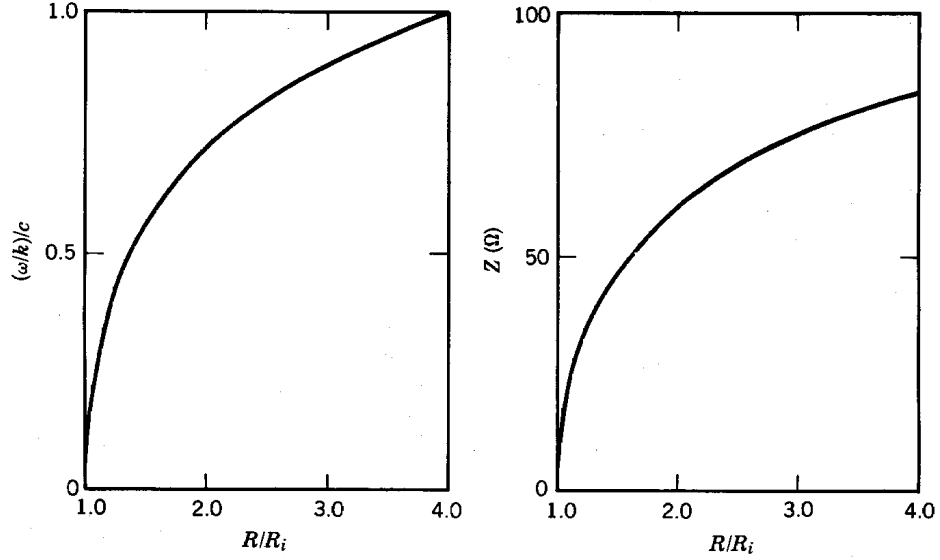


Figure 12.19 Phase velocity and characteristic impedance of capacitively loaded transmission line as function of R/R_i . ($\epsilon = \epsilon_0$, $R_i/R_0 = 0.25$).

$$C = 2\pi\epsilon / \ln(R/R_i). \quad (12.108)$$

The phase velocity as a function of R/R_0 is

$$\omega/k \cong c \sqrt{\ln(R/R_i) / \ln(R_0/R_i)}. \quad (12.109)$$

The characteristic impedance for TEM waves becomes

$$Z = \sqrt{L/C} = Z_0 \sqrt{\ln(R_0/R_i) / \ln(R/R_i)}. \quad (12.109)$$

The phase velocity and characteristic impedance are plotted in Figure 12.19 as a function of R/R_i . Note the following features:

1. The phase velocity decreases with increasing volume enclosed between the irises.
2. The phase velocity is less than the speed of light.
3. The characteristic impedance decreases with smaller iris inner radius.

Resonant Cavities and Waveguides

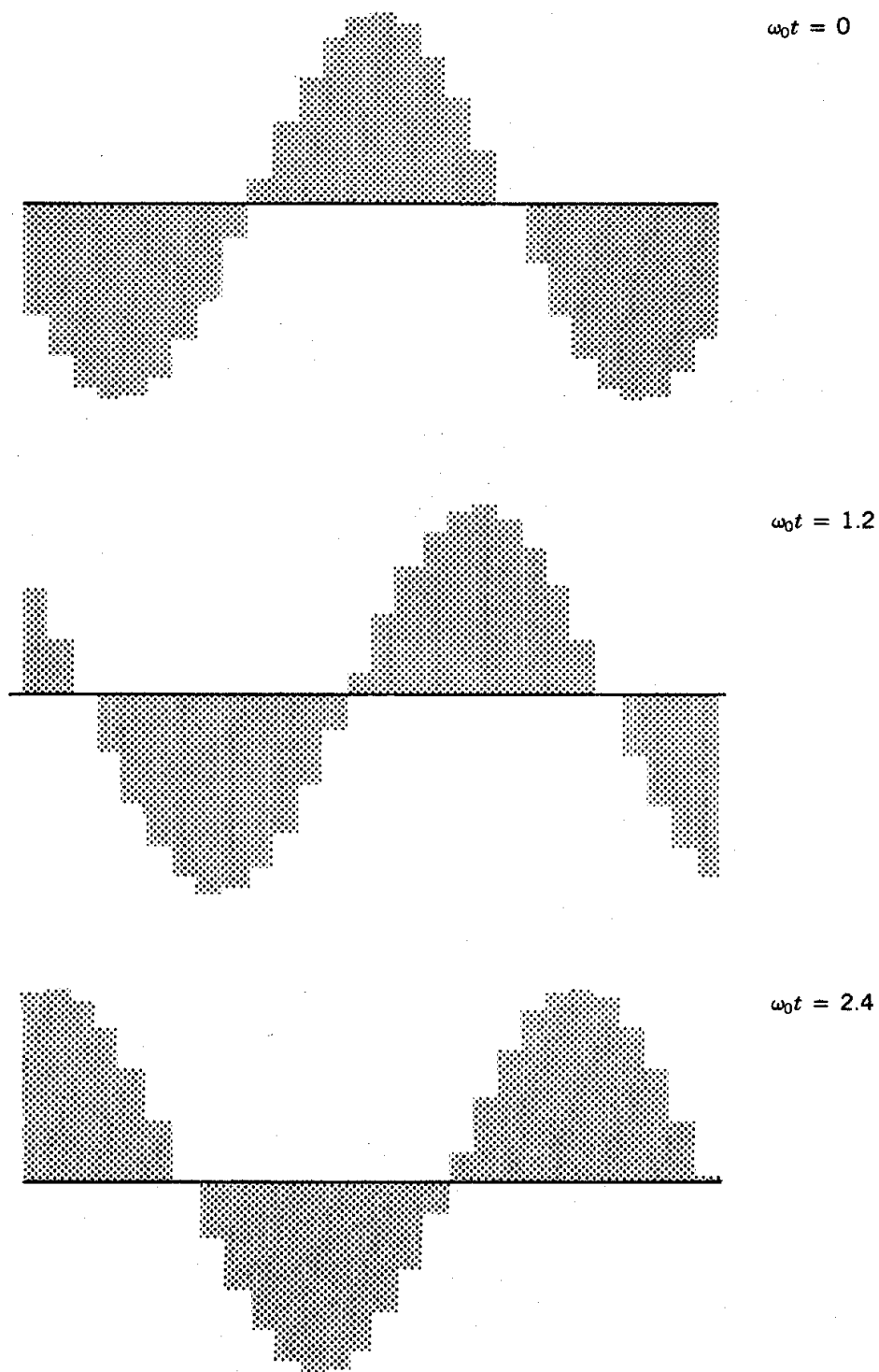


Figure 12.20 Electric field amplitudes in array of individually phased resonant cavities (27 cavities, with oscillations separated by constant phase difference $\Delta\phi = -0.3$ rad). Plots at times given by $\omega_0 t = 0, 1.2, 2.4, 3.6, 4.8, 6$.

Resonant Cavities and Waveguides

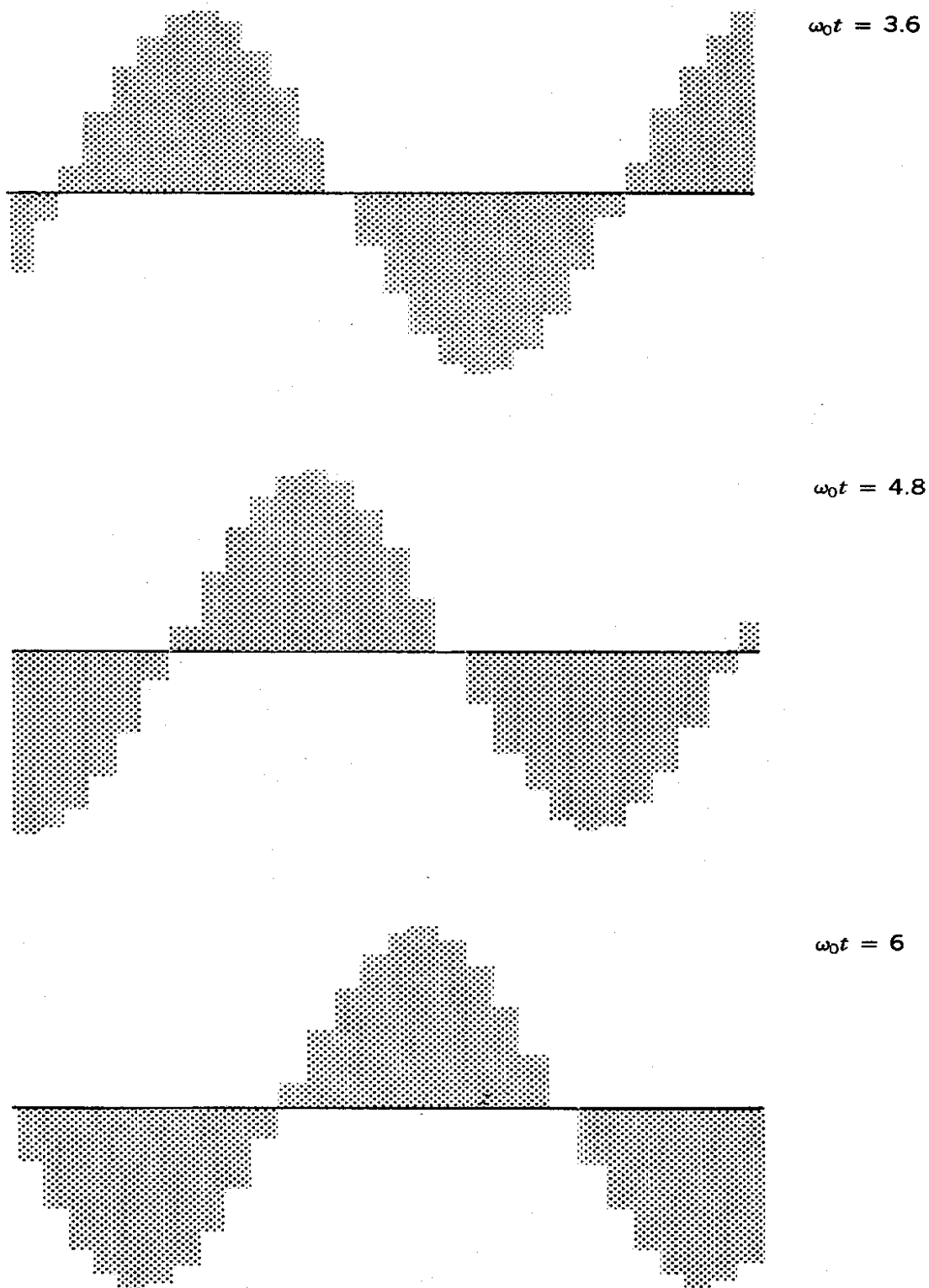


Figure 12.20 (Continued).

Resonant Cavities and Waveguides

4. In the long wavelength limit ($\lambda \gg \delta$), the phase velocity is independent of frequency. This is not true when $\lambda \leq \delta$. A general treatment of the capacitively loaded transmission line is given in Section 12.10.

A similar approach can be used to describe propagation of TM_{01} modes in an iris-loaded waveguide (Fig. 12.18c). At long wavelength the inductance L_1 is almost unchanged by the presence of irises, but the capacitances C_1 and C_2 of the lumped element model is increased. The phase velocity is reduced. Depending on the geometry of the irises, the phase velocity may be pulled below c . Capacitive loading also reduces the cutoff frequency ω_c . In the limit of strong loading ($R \ll R_0$), the cutoff frequency for TM_{01} waves approaches the frequency of the TM_{010} mode in a cylindrical resonant cavity of radius R_0 .

The following model demonstrates how the irises of a loaded waveguide produce the proper boundary fields to support an electrostatic field pattern in the rest frame of a slow wave. Consider an iris-loaded waveguide in the limit that $R \ll R_0$ (Fig. 12.18c). The sections between irises are similar to cylindrical resonant cavities. A traveling wave moves along the axis through the small holes; this wave carries little energy and has negligible effect on the individual cavities. Assume that cavities are driven in the TM_{010} mode by external power feeds; the phase of the electromagnetic oscillation can be adjusted in each cavity. Such a geometry is called an *individually phased cavity array*. In the limit $\lambda \gg \delta$, the cavity fields at R are almost pure E_z fields. These fields can be matched to the longitudinal electric field of a traveling wave to determine the wave properties.

Assume that δ is longitudinally uniform and that there is a constant phase difference $-\Delta\phi$ between adjacent cavities. The input voltage has frequency $\omega \approx 2.405c/R_0$. Figure 12.20 is a plot of electric field at R in a number of adjacent cavities separated by a constant phase interval at different times. Observe that the field at a particular time is a finite difference approximation to a sine wave with wavelength

$$\lambda = 2\pi\delta/\Delta\phi. \quad (12.111)$$

Comparison of plots at different times shows that the waveform moves in the $+z$ direction at velocity

$$v(\text{phase}) = \omega/k = (2.405/\Delta\phi) (\delta/R_0) c. \quad (12.112)$$

The phase velocity is high at long wavelength. A slow wave results when

$$\Delta\phi \geq 2.405 \delta/R_0 \quad \text{or} \quad \lambda < R_0/2.405. \quad (12.113)$$

In the rest frame of a slow wave, the boundary electric fields at R approximate a static sinusoidal field pattern. Although the fields oscillate inside the individual cavities between irises, the electric field at R appears to be static to an observer moving at velocity ω/k . Magnetic fields are confined within the cavities. The reactive boundaries, therefore, are consistent with an axial variation of electrostatic potential in the wave rest frame.

12.10 DISPERSION RELATIONSHIP FOR THE IRIS-LOADED WAVEGUIDE

The dispersion relationship $\omega = \omega(k)$ is an equation relating frequency and wavenumber for a propagating wave. In this section, we shall consider the implications of dispersion relationships for electromagnetic waves propagating in metal structures. We are already familiar with one quantity derived from the dispersion relationship, the phase velocity ω/k . The group velocity v_g is another important parameter. It is the propagation velocity for modulations of frequency or amplitude. Waves with constant amplitude and frequency cannot carry information; information is conveyed by changes in the wave properties. Therefore, the group velocity is the velocity for information transmission. The group velocity is given by

$$v_g = d\omega/dk. \quad (12.114)$$

Equation (12.114) can be derived through the calculation of the motion of a pulsed disturbance consisting of a spectrum of wave components. The pulse is Fourier analyzed into frequency components; a Fourier synthesis after a time interval shows that the centroid of the pulse moves if the wavenumber varies with frequency.

As an example of group velocity, consider TEM electromagnetic waves in a transmission line. Frequency and wavenumber are related simply by $\omega = k/\sqrt{\epsilon\mu} = kv$. Both the phase and group velocity are equal to the speed of light in the medium. There is no dispersion; all frequency components of a pulse move at the same rate through the line; therefore, the pulse translates with no distortion. Waves in waveguides have dispersion. In this case, the components of a pulse move at different velocities and a pulse widens as it propagates.

The group velocity has a second important physical interpretation. In most circumstances, the group velocity is equal to the flux of energy in a wave along the direction of propagation divided by the electromagnetic energy density. Therefore, group velocity usually characterizes energy transport in a wave.

Dispersion relationships are often represented as graphs of ω versus k . In this section, we shall construct ω - k plots for a number of wave transport structures, including the iris-loaded waveguide. The straight-line plot of Figure 12.21a corresponds to TEM waves in a vacuum transmission line. The phase velocity is the slope of a line connecting a point on the dispersion curve to the origin. The group velocity is the slope of the dispersion curve. In this case, both velocities are equal to c at all frequencies.

Figure 12.21b shows an ω - k plot for waves passing along the axis of an array of individually phased circular cavities with small coupling holes. The curve is plotted for an outer radius of $R_0 = 0.3$ m and a distance of 0.05 m between irises. The frequency depends only on the cavity properties not the wavelength of the weak coupling wave. Only discrete frequencies corresponding to cavity resonances are allowed. The reactive boundary conditions for azimuthally symmetric slow waves can be generated by any TM_{0n0} mode. Choice of the relative phase, $\Delta\phi$, determines k for the propagating wave. Phase velocity and group velocity are indicated in Figure 12.21b. The line

Resonant Cavities and Waveguides

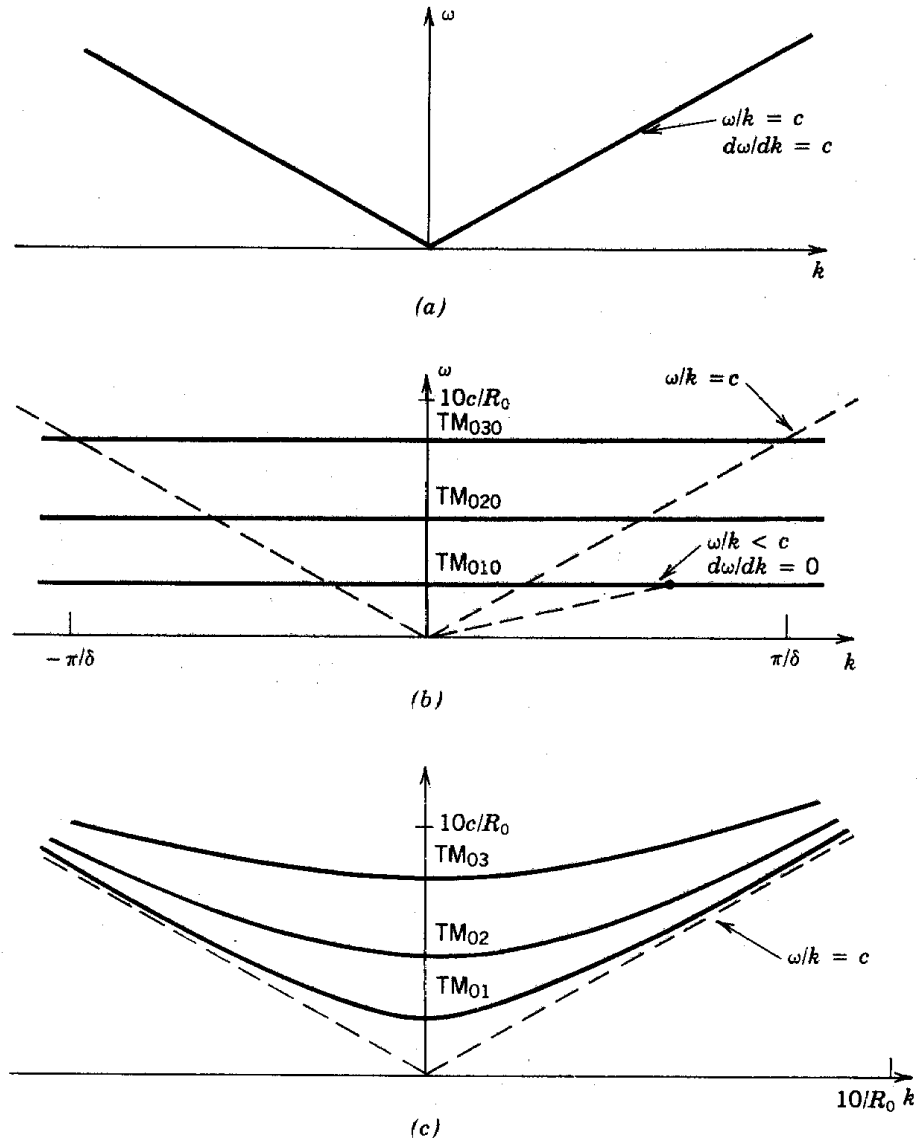


Figure 12.21 Dispersion relationships. (a) TEM waves in a transmission line. (b) Weakly coupled waves between individually phased cavities with constant phase difference, TM_{0n0} cavity modes. Point indicates possible conditions for a slow wave. (c) TM_{0n} modes in a circular waveguide.

corresponding to $\omega/k = c$ has also been plotted. At short wavelengths (large k), the phase velocity can be less than c . Note that since ω is not a function of k , the group velocity is zero. Therefore, the traveling wave does not transport energy between the cavities. This is consistent with the assumption of small coupling holes. The physical model of Section 12.8 is not applicable for wavelengths less than 2δ ; this limit has also been indicated on the ω/k graph.

The third example is the uniform circular waveguide. Figure 12.21c shows a plot of Eq. (12.103)

Resonant Cavities and Waveguides

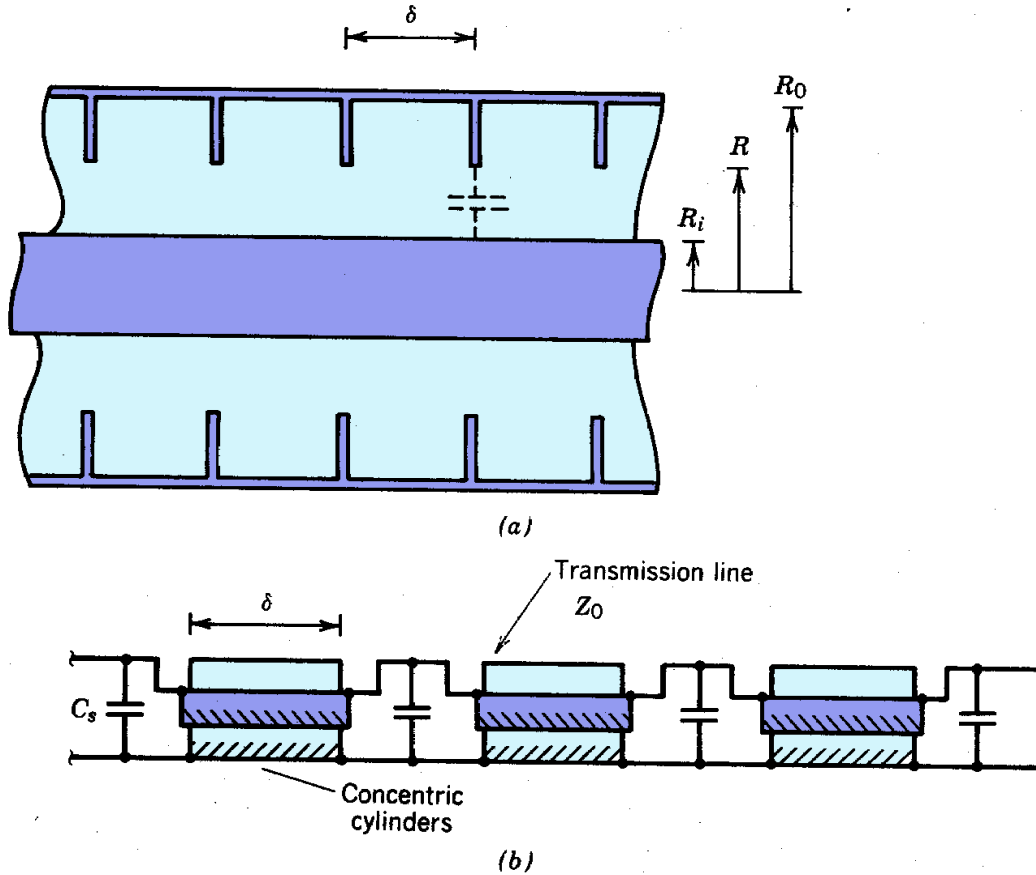


Figure 12.22 Modeling capacitively loaded transmission line as uniform transmission line with periodic shunt capacitance. (a) Geometry. (b) Equivalent circuit.

for a choice of $R_0 = 0.3$ m. Curves are included for the TM_{01} , TM_{02} , and TM_{03} modes. Observe that wavenumbers are undefined for frequency less than ω_c . The group velocity approaches zero in the limit that $\omega \Rightarrow \omega_c$. When $\omega = \omega_c$ energy cannot be transported into the waveguide because $k = 0$. The group velocity is nonzero at short wavelengths (large k). The boundaries have little effect when $\lambda \ll R$; in this limit, the ω - k plot approaches that of free-space waves, $\omega/k = c$. At long wavelength (small k), the oscillation frequencies approach those of TM_{0n0} modes in an axially bounded cavity with radius R . The phase velocity in a waveguide is minimum at long wavelength; it can never be less than c .

As a fourth example, consider the dispersion relationship for waves propagating in the capacitively loaded transmission line of Figure 12.22a. This example illustrates some general properties of waves in periodic structures and gives an opportunity to examine methods for analyzing periodic structures mathematically. The capacitively loaded transmission line can be considered as a transmission line with periodic impedance discontinuities. The discontinuities arise from the capacitance between the irises and the center conductor. An equivalent circuit is shown in Figure 12.22b; it consists of a series of transmission lines of impedance Z_0 and length δ with a

Resonant Cavities and Waveguides

shunt capacitance C_s at the junctions. The goal is to determine the wavenumber of harmonic waves propagating in the structure as a function of frequency. Propagating waves may have both positive-going and negative-going components.

Equations (12.68) and (12.69) can be used to determine the change in the voltage and current of a wave passing through a section of transmission line of length δ . Rewriting Eq. (12.68),

$$\begin{aligned} V(z+\delta) &= V_+ \exp(-j\omega\delta/v) + V_- \exp(j\omega\delta/v) \\ &= (V_+ + V_-) \cos(\omega\delta/v) - j(V_+ - V_-) \sin(\omega\delta/v) \\ &= V(z) \cos(\omega\delta/v) - jZ_o I(z) \sin(\omega\delta/v). \end{aligned} \quad (12.115)$$

The final form results from expanding the complex exponentials [Eq. (12.5)] and applying Eqs. (12.66) and (12.67). A time variation $\exp(j\omega t)$ is implicitly assumed. In a similar manner, Eq. (12.69) can be modified to

$$I(z+\delta) = I(z) \cos(\omega\delta/v) - jV(z) \sin(\omega\delta/v)/Z_o. \quad (12.116)$$

Equations (12.115) and (12.116) can be united in a single matrix equation,

$$\begin{pmatrix} V(z+\delta) \\ I(z+\delta) \end{pmatrix} = \begin{bmatrix} \cos(\omega\delta/v) & -jZ_o \sin(\omega\delta/v) \\ -j \sin(\omega\delta/v)/Z_o & \cos(\omega\delta/v) \end{bmatrix} \begin{pmatrix} V(z) \\ I(z) \end{pmatrix} \quad (12.117)$$

The shunt capacitance causes the following changes in voltage and current propagating across the junction:

$$V' = V(z+\delta), \quad (12.118)$$

$$I' = I(z+\delta) - j\omega C_s V(z+\delta). \quad (12.119)$$

In matrix notation, Eqs. (12.118) and (12.119) can be written,

$$\begin{pmatrix} V' \\ I' \end{pmatrix} = \begin{bmatrix} 1 & 0 \\ -j\omega C_s & 1 \end{bmatrix} \begin{pmatrix} V(z+\delta) \\ I(z+\delta) \end{pmatrix}. \quad (12.120)$$

The total change in voltage and current passing through one cell of the capacitively loaded transmission line is determined by multiplication of the matrices in Eqs. (12.117) and (12.120):

Resonant Cavities and Waveguides

$$\begin{pmatrix} V' \\ I' \end{pmatrix} = \begin{bmatrix} \cos(\omega\delta/v) & -jZ_o \sin(\omega\delta/v) \\ -j[\omega C_s \cos(\omega\delta/v) + \sin(\omega\delta/v)/Z_o] & \cos(\omega\delta/v) - \omega C_s Z_o \sin(\omega\delta/v) \end{bmatrix} \begin{pmatrix} V \\ I \end{pmatrix} \quad (12.117)$$

Applying the results of Section 8.6, the voltage and current at the cell boundaries vary harmonically along the length of the loaded transmission line with phase advance given by $\cos\mu = \text{Tr}\mathbf{M}/2$, where \mathbf{M} is the transfer matrix for a cell [Eq. (12.121)]. If k is the wavenumber of the propagating wave, the phase advance over a cell of length δ is $\mu = k\delta$. Taking the trace of the matrix of Eq. (12.121) gives the following dispersion relationship for TEM waves in a capacitively loaded transmission line:

$$\cos(k\delta) = \cos(\omega\delta/v) - (C_s Z_o v/2\delta) (\omega\delta/v) \sin(\omega\delta/v). \quad (12.122)$$

Equation (12.122) is plotted in Figure 12.23 for three choices of $(C_s Z_o v/2\delta)$. In the limit of no loading ($C_s = 0$), the dispersion relationship reduces to that of an unloaded line; both the group and phase velocities equal v (the velocity of light in the medium filling the line). With loading, the phase velocity is reduced below v (slow waves). The long wavelength (small k) results agree with the analysis of Section 12.9; the phase velocity and group velocity are independent of frequency. The wave characteristics deviate considerably from those of a TEM wave in an unloaded line when k approaches π/δ . The group velocity approaches zero when $\lambda/2 \Rightarrow \delta$. In this case, the wave is a standing-wave pattern with equal components of positive-going and negative-going waves. The feature is explained below in terms of constructive interference of wave reflections from the line discontinuities. The form of Eq. (12.122) implies that the dispersion plot repeats periodically for higher values of wavenumber.

The final example of a dispersion curve is the iris-loaded waveguide. The ω - k diagram is important in designing traveling wave particle accelerators; the phase velocity must match the particle velocity at all points in the accelerator, and the group velocity must be high enough to transport power through the structure effectively. In this calculation, we will determine how the size of the aperture (R) affects a TM_{01} wave moving through the coupling holes. We will limit attention to the long wavelength limit ($\lambda > 2\delta$). The iris spacing and outer radius are assumed constant. We have already treated two special cases, $R/R_0 = 1$ (uniform circular waveguide) and $R/R_0 = 0$ (independently phased array). Curves for these limits are plotted on Figure 12.24. Consider an intermediate case such as $R/R_0 = 0.5$. At long wavelength, inspection of the curves for the limiting cases infers that the frequency approaches $\omega = 2.405c/R_0$. This behavior can be understood if we consider a long wavelength TM_{01} mode in an ordinary waveguide of radius R_0 . The magnetic field is azimuthal, while the electric field is predominantly axial. The addition of thin irises has negligible effect on the electric and magnetic field lines because the oscillating fields induce little net current flow on the irises. In the long wavelength limit, electric fields of the TM_{01} mode are relatively unaffected by the radial metal plates. Current flow induced on the irises by oscillating magnetic field is almost equal and opposite on the upstream and downstream sides. The

Resonant Cavities and Waveguides

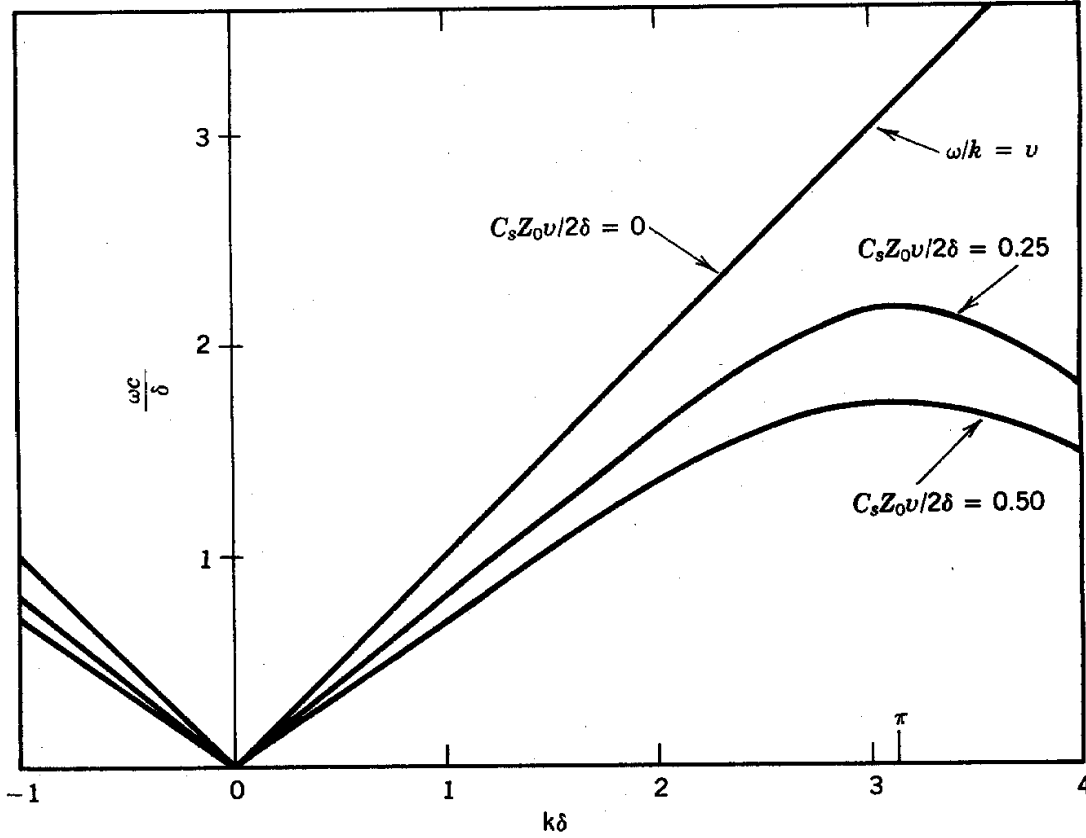


Figure 12.23 Dispersion relationship for capacitively loaded transmission line as function of $C_s Z_0 v / 2\delta$. C_s , shunt capacitance between iris and inner conductor; Z_0 , characteristic impedance of uniform line; v , speed of light in line medium; δ , distance between irises.

only effect is exclusion of magnetic field from the interior of the thin irises.

We can understand the ω - k diagram at short wavelengths by approximating the wave as a free-space plane wave. The irises represent discontinuities in the waveguide along the direction of propagation; some of the wave energy may be reflected at the discontinuity. Depending on the geometry, there is the possibility of constructive interference of the reflected waves. To understand this, assume that transmitted and reflected waves are observed at the point $z = 0$. Irises are located at distances $\delta, 2\delta, 3\delta, \dots, n\delta$ downstream. A waveform reaches a particular iris at a time $n\delta/(\omega/k)$ after it passes the point $z = 0$. A reflected wave from the iris takes a time $n\delta/(\omega/k)$ to return to the origin. The sum of reflected waves at $z = 0$ is therefore

$$E_z(\text{reflected}) \sim \sum \exp[j(\omega t - 2\pi\delta k)] = \sum \exp(j\omega t) \cos(2n\delta k). \quad (12.123)$$

Resonant Cavities and Waveguides

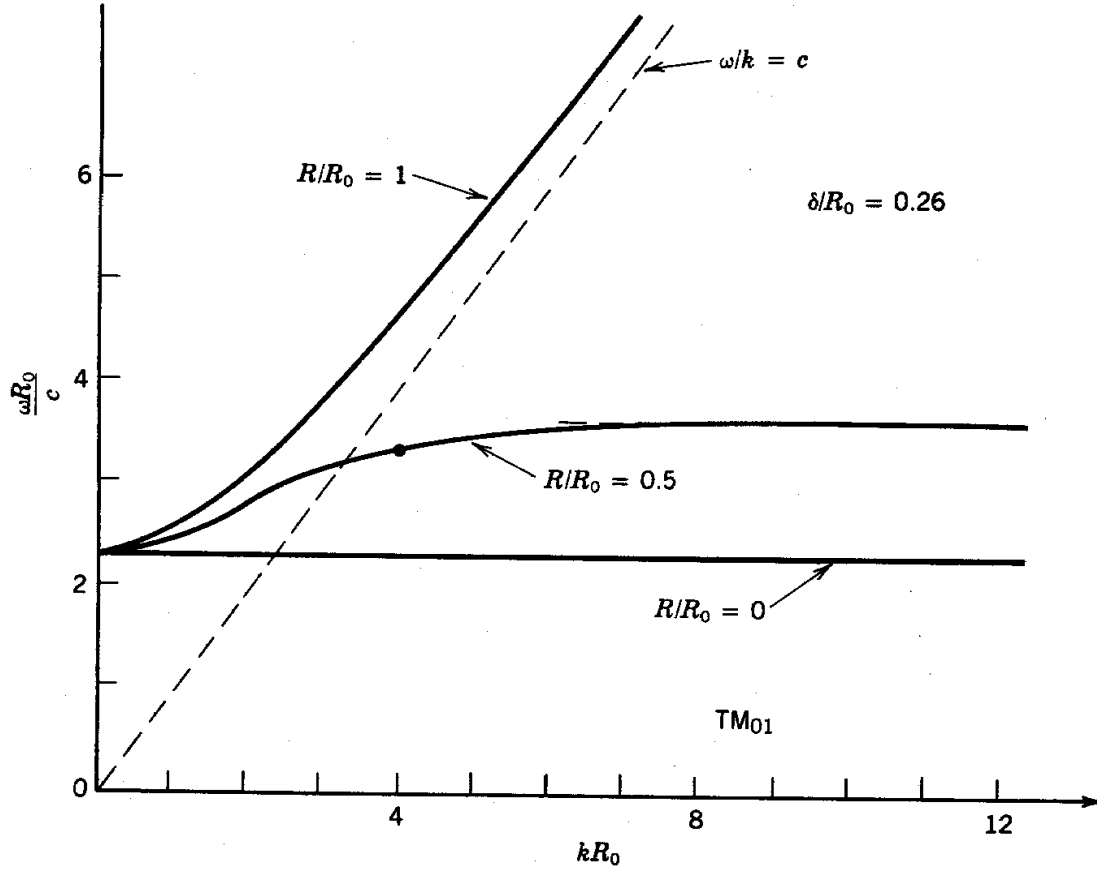


Figure 12.24 Dispersion relationships in the range $0 \leq k \leq \pi/\delta$ for TM_{01} mode propagation in iris-loaded waveguide of radius R_0 as a function of inner radius of iris, R . $R/R_0 = 0$ corresponds to individually phase cavities, $R/R_0 = 1$ corresponds to circular waveguide. Point indicates slow wave with nonzero group velocity.

The summation of Eq. (12.123) diverges when $k = \pi/\delta$. In this case, there is a strong reflected wave. The final state has equipartition of energy between waves traveling in the $+z$ and $-z$ directions; therefore, a standing-wave pattern with zero group velocity is set up.

We can estimate the frequency of the standing wave at $k = \pi/\delta$ by calculating the resonant frequency of a hollow annular cavity with specified inner radius. In the limit $\delta \ll (R_o - R_i)$, resonant frequencies of TM_{0n0} modes are determined by solving Eq. (12.42) with boundary conditions $E_z(R_o) = 0$ and $B_\theta(R) = 0$. The latter condition comes about because the axial displacement current between $r = 0$ and $r = R$ is small. The boundary condition can be rewritten as $dE_z(R)/dr = 0$. The resonant frequencies are determined by the solutions of the transcendental equation:

Resonant Cavities and Waveguides

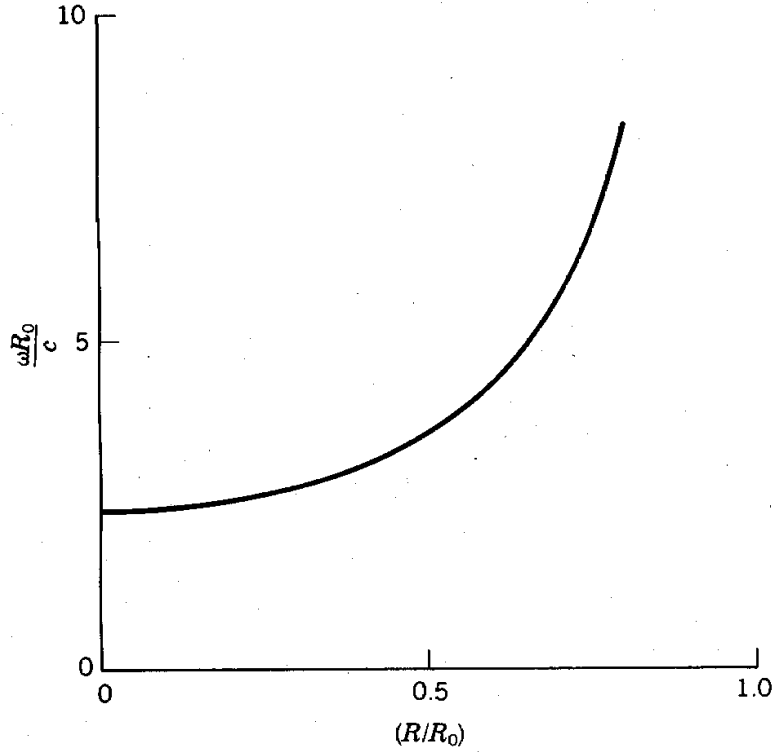


Figure 12.25 Frequency of TM_{010} mode as function of R/R_0 in annular cavity with length d , outer radius R_0 , and inner radius R . Open circuit boundary at inner radius; $\delta \ll R$.

$$\frac{J_1(\omega R/c) Y_0(\omega R_0/c)}{J_0(\omega R_0/c) Y_1(\omega R/c)} = 1 \quad (12.124)$$

Resonant frequencies as a function of R/R_0 are plotted in Figure 12.25 for the TM_{01} and TM_{02} modes. For our example [$R/R_0 = 0.5$], the frequency of the hollow cavity is about 50% higher than that of the complete cavity. This value was incorporated in the plot of Figure 12.24.

Consider some of the implications of Figure 12.24. In the limit of small coupling holes, the cavities are independent. We saw in discussing individually phased cavities that phase velocities much less than the speed of light can be generated by the proper choice of the phasing and δ/R . Although there is latitude to achieve a wide range of phase velocity in the low coupling limit, the low group velocity is a disadvantage. Low group velocity means that energy cannot be coupled between cavities by a traveling wave.

The interdependence of phase and group velocity in a periodic structure enters into the design of rf linear accelerators (Chapter 14). In an accelerator for moderate- to high-energy electrons, the phase velocity is close to c . Inspection of Figure 12.24 shows that this value of phase velocity can

Resonant Cavities and Waveguides

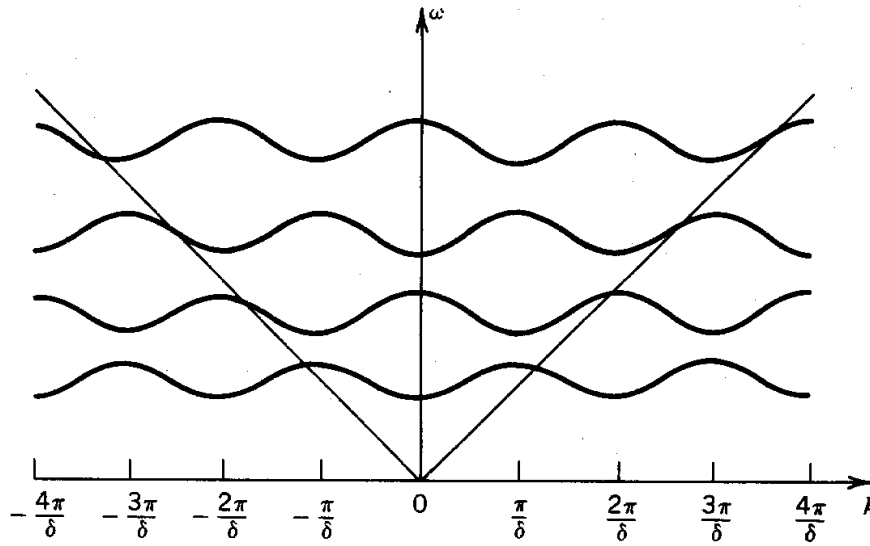


Figure 12.26 Brillouin diagram of wave properties in a capacitively loaded cylindrical waveguide with iris spacing δ .

be achieved in a structure with substantial coupling holes and a high value of group velocity. This means that a useful traveling wave can be excited in an extended structure with nonzero wall resistivity by a single power input. The boundary cavities between irises are excited by energy carried by the traveling wave. This approach is not suitable for linear ion accelerators, where the phase velocity must be well below the speed of light. This is the reason linear ion accelerators generally use external rf coupling of individual cavities to synthesize a slow traveling wave on axis.

In the above derivation, we concentrated on TM_{01} waves over the wavenumber range $0 < k < \pi/\delta$. This is the range generally encountered in accelerator applications. We should recognize, nonetheless, that higher-order modes and traveling waves with $\lambda < 2\delta$ can be propagated. The complete ω - k plot for a periodic waveguide structure is called a *Brillouin diagram* [L. Brillouin. **Wave Propagation in Periodic Structures**, Dover, New York, 1953]. An example is illustrated in Figure 12.26. The periodic repetition of the curve along the k axis is a consequence of the axial periodicity of the waveguide structure. Note the similarities between Figure 12.26 and the dispersion relationship for TEM waves in the capacitively loaded transmission line (Fig. 12.22).